

Low-Density Graph Codes for slow fading Relay Channels

Dieter Duyck, Joseph J. Boutros, and Marc Moeneclaey

Abstract

We study Low-Density Parity-Check (LDPC) codes with iterative decoding on block-fading (BF) Relay Channels. We consider two users that employ coded cooperation, a variant of decode-and-forward with a smaller outage probability than the latter. An outage probability analysis for discrete constellations shows that full-diversity can be achieved only when the coding rate does not exceed a maximum value that depends on the level of cooperation. We derive a new code structure by extending the previously published full-diversity root-LDPC code, designed for the BF point-to-point channel, to exhibit a rate-compatibility property which is necessary for coded cooperation. Word error rate (WER) performance is determined for infinite length codes through density evolution (DE) as well as for finite length codes. We show that our code construction exhibits near-outage limit performance for all block lengths and for a range of coding rates up to 0.5, which is the highest possible coding rate for two cooperating users.

Index Terms

Relay channels, fading channels, binary erasure channel, low-density parity-check code, mutual information, density evolution.

Dieter Duyck and Marc Moeneclaey are with the Department of Telecommunications and Information processing, Ghent University, St-Pietersnieuwstraat 41, B-9000 Gent, Belgium, {dduyck,mm}@telin.ugent.be. Joseph J. Boutros is with Texas A&M University at Qatar, PO Box 23874 Doha, Qatar, boutros@tamu.edu

The authors wish to acknowledge the activity of the Network of Excellence in Wireless COMMunications NEWCOM++ of the European Commission (contract no. 216715) that motivated this work.

I. INTRODUCTION

When communicating over fading channels, Word Error Rate (WER) performances as well as power savings are dramatically improved through transmit diversity, i.e., transmitting signals carrying the same information over different paths in time, frequency or space. Spatial diversity obtained by the transmitter generally requires a Multiple Input (multiple antennas) system. However, many wireless devices have constraints in size or hardware complexity so that they can be equipped with only one antenna. Recently, a new network protocol called *Cooperative Communication* [11], [22], [29], [36], [37] yields transmit diversity using single-antenna devices in a multi-user environment by taking advantage of the broadcast nature of wireless transmission. The most elementary example of a cooperative network is the relay channel, introduced by van der Meulen [28]. In a relay channel, a relay helps the source in transmitting its data to a destination by relaying the messages sent by the source so that the received energy at the destination is increased. This relay channel can be generalized to a cooperative Multiple Access Channel (MAC) [22], where two users transmitting data to a single receiver cooperate by alternately being the relay for the other user, as indicated in Fig. 1. Further generalization to more users is possible, but this will not be discussed here for simplicity. Cooperative communications with practical algorithms in a wireless context was first shown to have a higher throughput than direct transmission by Sendonaris et al. [36], [37].

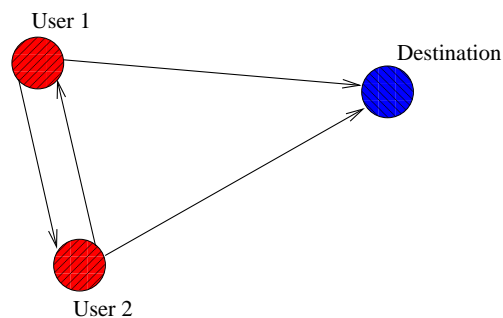


Fig. 1. A Cooperative Multiple Access Channel (MAC). Arrows between two nodes illustrate that both nodes communicate between each other.

A challenging channel model is the BF [4] frequency non-selective Single-Input Single-Output (SISO) channel. When the fading gain is constant over a codeword and no cooperation is used,

the resulting word error rate curve (displaying the logarithm of the error rate versus the average signal-to-noise ratio (SNR) in dB) has the same high-SNR slope as for uncoded transmission: the corresponding diversity order¹ equals one. In this case, a lot of transmit energy is needed to achieve sufficiently low error-rates. Automatic Repeat-reQuest (ARQ) is one of the means to increase the diversity, at the expense of increased packet delay. The potential diversity increase brought by cooperative techniques allows to save much transmit energy at a given error rate and to reduce the delay of the received packet due to less retransmission requests. This channel model is adopted here because of the large promised gains due to cooperation. BF channels are a realistic model for a number of channels affected by slowly varying fading and flat fading is assumed in order to isolate the effect of cooperative diversity.

The specific task of the relay is determined by the strategy or protocol. In the case of Amplify and Forward (AF), the relay amplifies the received signal and noise; for Decode and Forward (DF), the relay first decodes and then re-encodes the message before sending it to the destination. It is not straightforward to state which strategy is optimal, because this depends on the channel conditions, such as the ergodicity of the temporal correlation of the fading gain and the distances between the source, the relay and the destination [21]. A variant of DF is coded cooperation, where the relay decodes the message received from the source, and then transmits *additional* parity bits of the message, resulting in a more spectral efficient strategy [18], compared to a traditional DF protocol. Instead of *SNR accumulation* (logarithmic rise of mutual information with received power from the relay) at the destination, we get *information accumulation* (linear rise of mutual information with received power from the relay) [42]. It has been shown in [19] that the outage probability [4], [30] of coded cooperation for half-duplex BF channels is smaller than for repetition-based protocols. Moreover, the concept of coded cooperation can be used in more complex strategies, such as Amplify-Decode-Forward [2], where the relay can choose between DF and AF. So finally, replacing the decode-and-repeat part in any protocol by this more intelligent “information adding” strategy improves the outage probability performance. As a consequence, constructing a near-outage channel code for a coded cooperation scenario results

¹Here, diversity order is defined as the ratio of the high-SNR slopes of the error rate curves of the considered system and of the uncoded system, respectively. Alternatively, diversity order can be defined as the slope of the error-rate curve of the considered system. The diversity depends on the fading gain distribution in the latter definition, but not in the former definition. Both definitions are equal in the case of Rayleigh fading.

in a competitive error-correcting code in terms of error-rate performance vs. SNR for a given rate R .

In a first part, this paper analyzes the outage probability for binary phase shift keying (BPSK) modulations and derives a coding rate limitation that is necessary for the protocol to have diversity two, valid for all discrete alphabets. But not every code satisfying this information theoretical rate limitation achieves a double diversity order. In contrast to DF, the diversity order is not guaranteed by the protocol itself. Deriving a code structure exhibiting full-diversity will be treated in the second part of the paper.

Up till now, coded cooperation has mainly been implemented using rate-compatible convolutional codes [18]. The main drawback of these codes is that the WER increases with the logarithm of block length to the power d where d is the diversity order [7], [8]. The WER of practical near-outage codes should be independent of the block length in order to approach the outage probability limit [12], [13]. The solution is to use capacity-achieving codes, such as LDPC codes [32] or Turbo Codes [3]. In this paper, we concentrate on the family of LDPC codes. LDPC codes designed for the special case of a cooperative channel have been reported by Razaghi et al. [31] for the Gaussian channel. For the block-fading channel however, there is still a lack of a near-outage LDPC code. Hu et al. [16] obtained interesting results by designing random LDPC codes for cooperation over fading channels, but they did not tune the parity-check matrix in order to achieve full-diversity, as shown by Boutros et al. [6] and as will be explained in the rest of the paper. The aim of coded cooperation is to send a codeword over two independent fading paths and the relay must be able to decode after receiving the first part of the codeword. An error-correcting code must therefore exhibit two properties: full-diversity and rate-compatibility. This paper derives a new code structure satisfying both properties. We also determine density evolution equations to study the performance of an infinite length LDPC code. These results are representative for finite length codes [32] as illustrated in the numerical results.

Channel-State Information (CSI) is assumed at the decoder. We consider half-duplex devices, assuming that simultaneously receiving and transmitting data in the same frequency-band is too complicated due to the limited isolation of directional couplers. In addition, we also restrict the protocol to be orthogonal since we transmit at low rates (we use Binary Phase-Shift Keying

(BPSK)). The proposed code construction can nevertheless be used in more complex non-orthogonal protocols, where one can achieve more coding gain in high-rate scenarios [1].

II. SYSTEM MODEL AND NOTATION

As mentioned in the introduction, the devices are half-duplex and users transmit in non-overlapping time slots. The transmission of a codeword is organized in two frames which constitute one block. We denote the transmission of user u , $u = 1, 2$, in frame m , $m = 1, 2$, by $X_{u,m}$. The pairs $(C_{u,1}, C_{u,2})$ denote the codewords of user u . In the first frame of a block, each user broadcasts the first part of its encoded data to the other user and to the destination. In the second frame, users either cooperate or send additional parity bits related to their own information message, depending on whether they are able to decode the transmissions in the first frame. The decoding failure is detected by the relaying user via a Cyclic Redundancy Check (CRC) code or any other intelligent detection scheme. There are 4 cases to be distinguished, as summarized in Fig. 2: in case 1, both users have successfully decoded the information from the other user; in case 2, none of the users has been able to decode the information from the other user; in case 3 (case 4), only user 2 (user 1) has successfully decoded the information from the other user. Two methods have been proposed in [17] allowing the destination to detect which of these 4 cases has occurred: (i) The first method is to decode according to all possible assumptions until CRCs indicate successful decoding, (ii) The second method is to let each user transmit one additional bit to indicate its state to the receiver.

A codeword will consequently be split over 2 frames. We consider codewords to have a total length equal to N binary digits, where $N = N_1 + N_2$, and N_1 and N_2 denote the length of the first and second part of the codeword. We define the level of cooperation, β , as the ratio N_2/N . We denote the transmitter of a frame, which can be user 1 or user 2, by s and the receiver of a frame, which can be user 1, user 2 or the destination, by r . Transmitted symbols of user 1 will be denoted $x_1[i]$ where i is the symbol time index, $i \in \{1, \dots, N\}$. Similarly, transmitted symbols of user 2 are denoted $x_2[i]$. The transmitted symbols are chosen from a BPSK alphabet, $x_s[i] \in \{1, -1\}$. Received symbols will be denoted $y_{sr}[i]$ for received symbols from transmitter s to receiver r . The received symbol is given by

$$y_{sr}[i] = \alpha_{sr}x_s[i] + z_r[i], \quad (1)$$

	Frame 1		Frame 2	
User 1	$X_{1,1} = C_{1,1}$		$X_{1,2} = C_{2,2}$	
User 2		$X_{2,1} = C_{2,1}$		$X_{2,2} = C_{1,2}$

(a) Case 1. Both interuser transmissions are successfully decoded. Each user cooperates in the second frame.

	Frame 1		Frame 2	
User 1	$X_{1,1} = C_{1,1}$		$X_{1,2} = C_{1,2}$	
User 2		$X_{2,1} = C_{2,1}$		$X_{2,2} = C_{1,2}$

(c) Case 3. User2-to-User1 communication failed. In the second frame, user 1 sends its own parity bits and user 2 cooperates with user 1.

	Frame 1		Frame 2	
User 1	$X_{1,1} = C_{1,1}$		$X_{1,2} = C_{1,2}$	
User 2		$X_{2,1} = C_{2,1}$		$X_{2,2} = C_{2,2}$

(b) Case 2. Both interuser communications failed. Each user sends its own parity bits in the second frame.

	Frame 1		Frame 2	
User 1	$X_{1,1} = C_{1,1}$		$X_{1,2} = C_{2,2}$	
User 2		$X_{2,1} = C_{2,1}$		$X_{2,2} = C_{2,2}$

(d) Case 4. User1-to-User2 communicatino failed. In the second frame, user 2 sends its own parity bits and user 1 cooperates with user 2.

Fig. 2. The 4 cases encountered in coded cooperation are listed above.

where $z_r[i] \sim \mathcal{N}(0, \sigma^2)$ are independent noise samples and $\alpha_{sr} \in \mathbb{R}^+$ is the Rayleigh distributed fading gain between sender s and receiver r . The fading coefficient α_{sr} is assumed to be constant during 2 frames and is independent from block to block due to interleaving.

We focus on binary LDPC codes $\mathcal{C}[N, K]_2$ with block length N , dimension K , and coding rate $R_c = K/N$. The code \mathcal{C} is defined by an $(N - K) \times N$ parity-check matrix H , or equivalently, by the corresponding Tanner graph [5], [33]. It is assumed that H has full rank $(N - K)$, and consequently $R_c = 1 - \frac{N-K}{N}$. Regular LDPC ensembles are characterized by the pair (d_b, d_c) , where d_b is the maximum bitnode degree and d_c is the maximum checknode degree. Irregularity is introduced through the standard polynomials $\lambda(x)$ and $\rho(x)$ [34]:

$$\lambda(x) = \sum_{i=2}^{d_b} \lambda_i x^{i-1}, \quad \rho(x) = \sum_{i=2}^{d_c} \rho_i x^{i-1},$$

where λ_i (resp. ρ_i) is the fraction of all edges in the Tanner graph, connected to a bitnode (resp. checknode) of degree i . Therefore, $\lambda(x)$ and $\rho(x)$ are sometimes denoted as left and right degree distributions from an edge perspective. In section V the polynomials $\mathring{\lambda}(x)$ and $\mathring{\rho}(x)$, which are the left and right distributions from a node perspective, will also be adopted:

$$\mathring{\lambda}(x) = \sum_{i=2}^{d_b} \mathring{\lambda}_i x^{i-1}, \quad \mathring{\rho}(x) = \sum_{i=2}^{d_c} \mathring{\rho}_i x^{i-1},$$

where λ_i (resp. ρ_i) is the fraction of all bit nodes (resp. check nodes) in the Tanner graph of degree i , hence $\lambda_i = \frac{\lambda_i/i}{\sum_j \lambda_j/j}$ and likewise with ρ_i .

In this paper, not all bit nodes and check nodes in the Tanner graph will be treated equally. To elucidate the different classes of bit nodes and check nodes, a compact representation of the Tanner graph, adopted from [9] and also known as protograph representation [38], will be used. In this compact Tanner graph, bit nodes and check nodes of the same class are merged into one node.

The BF channel has a Shannon capacity that is essentially zero since the fading gain makes the mutual information a random variable which does not allow us to make the error probability arbitrarily small under a certain spectral efficiency. This word error probability is called *information outage probability* in the limit of large block length, denoted by

$$P_{out} = P(I(\alpha, \gamma) < R),$$

where $I(\alpha, \gamma)$ is the instantaneous mutual information as a function of a certain fading gain α and average SNR γ , $\gamma = \frac{E_s}{N_0} = \frac{1}{2\sigma^2}$, where E_s is the symbol energy. This definition remains valid for a channel model as described in (1), but then α is the set of fading gains over a codeword and γ is the set of average received SNRs. The rate R is the spectral efficiency of a user, only taking into account its timeslots, hence not the average spectral efficiency². It is our aim in this paper to approach the outage probability limit for a range of values of the spectral efficiency R . Since we use BPSK signaling, the spectral efficiency R is identical to R_c .

Definition 1 *The diversity order attained by a code \mathcal{C} is defined as*

$$d = - \lim_{\gamma \rightarrow \infty} \frac{\log P_e}{\log \gamma},$$

where P_e is the word error rate after decoding.

Definition 2 *An error-correcting code is said to have full-diversity if $d = N_u$, where N_u is the number of cooperating users.*

²This is, in our opinion, necessary for a fair comparison between multiple user networks with a different number of users.

Notice that the above definition assumes Rayleigh distributed single antenna channels. The diversity order of the outage probability limit is the same as the order attained by a full-diversity channel code [12]. According to the blockwise Singleton bound [20], [27], the coding rate for a n -order full-diversity code is upper bounded by $R_{cmax} = 1/n$. Hence, in a 2-user scenario we get $R_c \leq 0.5$.

III. OUTAGE PROBABILITY ANALYSIS

The outage probability analysis of coded cooperation with a Gaussian alphabet has been made in [19]. Here, the analysis considers BPSK signaling, leading to an important conclusion in Corollary 1 at the end of this section. The stated corollary is also valid for larger discrete alphabets.

The average mutual information of a SISO channel with received signal y , conditioned on the channel realization α , is determined by the following well-known formula [40]:

$$I(X; Y|\alpha) = 1 - \mathbb{E}_{Y|\alpha} \left\{ \log_2 \left(1 + \exp \left[\frac{-2y\alpha}{\sigma^2} \right] \right) \right\}, \quad (2)$$

where $\mathbb{E}_{Y|\alpha}$ is the mathematical expectation over Y given α . The outage event of a point-to-point link is defined by the mutual information of that link being less than its transmission rate. The outage event E_o of the relay channel is determined by a specific region in the multidimensional space of instantaneous signal-to-noise ratios. Next, we give the exact definition of E_o for coded cooperation with BPSK modulation. We shorten the notation $I(X_i; Y_j|\alpha_{ij})$ to I_{ij} .

Proposition 1 *In coded cooperation for a two-user MAC with BPSK signaling, the outage event E_o related to user 1 is expressed as follows:*

$$E_o \stackrel{a)}{=} \left\{ \begin{aligned} & [(I_{12} > R/(1-\beta)) \cap (I_{21} > R/(1-\beta)) \cap (I_{1d}(\text{case 1}) < R)] \\ & \cup [(I_{12} < R/(1-\beta)) \cap (I_{21} < R/(1-\beta)) \cap (I_{1d}(\text{case 2}) < R)] \\ & \cup [(I_{12} > R/(1-\beta)) \cap (I_{21} < R/(1-\beta)) \cap (I_{1d}(\text{case 3}) < R)] \\ & \cup [(I_{12} < R/(1-\beta)) \cap (I_{21} > R/(1-\beta)) \cap (I_{1d}(\text{case 4}) < R/(1-\beta))] \end{aligned} \right\}, \quad (3)$$

where

$$I_{12} \stackrel{b)}{=} 1 - \mathbb{E}_{Y|\alpha_{12}} \left\{ \log_2 \left(1 + \exp \left[\frac{-2y_{12}\alpha_{12}}{\sigma_{12}^2} \right] \right) \right\}, \quad (4)$$

$$I_{21} \stackrel{b)}{=} 1 - \mathbb{E}_{Y|\alpha_{21}} \left\{ \log_2 \left(1 + \exp \left[\frac{-2y_{21}\alpha_{21}}{\sigma_{21}^2} \right] \right) \right\}, \quad (5)$$

and where I_{1d} is case-dependent. For each of the cases considered in Fig. 2, the mutual information I_{1d} can be calculated as follows:

Case 1:

$$I_{1d} \stackrel{c)}{=} 1 - (1 - \beta) \mathbb{E}_{Y|\alpha_{1d}} \left\{ \log_2 \left(1 + \exp \left[\frac{-2y_{1d}\alpha_{1d}}{\sigma_{1d}^2} \right] \right) \right\} - \beta \mathbb{E}_{Y|\alpha_{2d}} \left\{ \log_2 \left(1 + \exp \left[\frac{-2y_{2d}\alpha_{2d}}{\sigma_{2d}^2} \right] \right) \right\}. \quad (6)$$

Case 2:

$$I_{1d} \stackrel{c)}{=} 1 - \mathbb{E}_{Y|\alpha_{1d}} \left\{ \log_2 \left(1 + \exp \left[\frac{-2y_{1d}\alpha_{1d}}{\sigma_{1d}^2} \right] \right) \right\}. \quad (7)$$

Case 3:

$$I_{1d} \stackrel{c)}{=} 1 - (1 - \beta) \mathbb{E}_{Y|\alpha_{1d}} \left\{ \log_2 \left(1 + \exp \left[\frac{-2y_{1d}\alpha_{1d}}{\sigma_{1d}^2} \right] \right) \right\} \\ - \beta \mathbb{E}_{Y'|\alpha_{1d}\alpha_{2d}} \left\{ \log_2 \left(1 + \exp \left[\frac{-2(y')(\alpha_{1d}^2 + \alpha_{2d}^2)^{3/2}}{\sigma_{1d}^2\alpha_{1d}^2 + \sigma_{2d}^2\alpha_{2d}^2} \right] \right) \right\}, \quad (8)$$

$$y' = \frac{(\alpha_{1d}y_{1d} + \alpha_{2d}y_{2d})}{\sqrt{\alpha_{1d}^2 + \alpha_{2d}^2}}.$$

Case 4:

$$I_{1d} \stackrel{c)}{=} 1 - \mathbb{E}_{Y|\alpha_{1d}} \left\{ \log_2 \left(1 + \exp \left[\frac{-2y_{1d}\alpha_{1d}}{\sigma_{1d}^2} \right] \right) \right\}. \quad (9)$$

Proof:

- a) is the union of four events associated to the four cases considered in Fig. 2. Each case in E_o involves the intersection with an outage event where the mutual information

between a user and the destination is below the rate R , except for case 4, where only the first frame is dedicated to user 1.

- b) follows directly from (2).
- c) uses the fact that the two frames in a block behave as parallel Gaussian channels whose capacities add together. Of course, both frames timeshare a time-interval, which gives a weight to each capacity term [10, Section 9.4], [39, Section 5.4.4].
- (8) follows from maximum ratio combining [39] at the destination during the second frame.

■

The outage probability is obtained by integrating the joint probability distribution $p(\alpha_{12}, \alpha_{21}, \alpha_{1d}, \alpha_{2d})$ over the volume defined by E_o . Just as for the Gaussian modulation, there is only one free parameter β because R and γ are fixed by the protocol and the physical environment. Hence, given R and γ , one can optimize the value of β . For example, notice that for a low-SNR interuser channel, the outage probability improves while taking β smaller than 0.5 due to the enhanced protection of the source-relay channel. On the other hand, a β smaller than 0.5 results in lower achievable coding rates, as proved in Corollary 1. The optimization of β , as already undertaken in [19] for Gaussian modulations, is not within the subject of this paper.

There is an important conclusion to draw from the analysis of Prop. 1:

Corollary 1 *In coded cooperation over a block-fading channel for the 2-user MAC with a cooperation level β , transmitting at a coding rate greater than $\min(\beta, (1 - \beta))$ renders a single order diversity.*

Proof: It is sufficient to prove the stated corollary for coded cooperation over a Block Erasure Channel (BEC) [24], because a BEC is an extremal case of a block-fading channel. In a BEC, the fading gain α takes two possible values $\{0, +\infty\}$. An outage event on a point-to-point channel is defined by the fading gain α being zero. As a consequence, the possible values of the BPSK capacity on a BEC are confined to zero or one. Hence, for the two-user MAC, the mutual information I_{1d} related to case 1 belongs to $\{1, \beta, (1 - \beta), 0\}$. A double diversity order is equivalent to stating that two outage events are necessary to lose the transmitted codeword. Take the scenario where the user1-to-destination channel has fading gain zero and the user2-to-destination channel has fading gain ∞ . In this scenario, the mutual information I_{1d} is equal to β . All coding rates higher than β will limit the diversity order of the outage probability to one,

since only one channel in outage is enough to lose the codeword. From a similar reasoning, it is shown that R_c must be smaller than $(1 - \beta)$. This corollary is also valid for signaling strategies with M constellation points. ■

In the sequel, if not otherwise stated, we assume a rate equal to $R_c = \frac{1}{3}$. From Corollary 1, we know that it is possible to have double diversity order for this rate if $\beta \in [\frac{1}{3}, \frac{2}{3}]$. We stress on the fact that the proposed code construction is very flexible in parameters such as the block length and the coding rate, as long as this coding rate is smaller than $\min(\beta, (1 - \beta))$. We will use $\beta = 0.5$ throughout this paper, which allows us to achieve diversity two for all rates R_c smaller than $1/2$. We illustrate this in the numerical results by showing the WER performance of an LDPC code whose coding rate R_c approaches $1/2$.

IV. FULL-DIVERSITY LOW-DENSITY CODING FOR CODED COOPERATION

Codewords in coded cooperation are split over 2 frames. The first part of a codeword, transmitted during the first frame should protect information on the noisy source-relay channel. Consequently, a channel code, compatible with two distinct rates is to be devised. In non-cooperative communications, this property is known as rate-compatibility where parity bits of higher rate codes are embedded in those of lower rate codes [15]. This concept was heavily used in the context of adaptive coding and unequal error protection in packet data communication. The advantage is that all codes can be encoded/decoded using a single encoder/decoder which is for example an efficient framework for ARQ/FEC, where incremental parity bits are transmitted in response to erroneous decoding at the receiver.

Rate-compatibility in the context of LDPC codes was first introduced by Li et al. [25] and Ha et al. [14] and further elaborated for example in [41]. Two techniques have been used: puncturing and extending. A fraction of parity bits of a mother code could be punctured to obtain higher rate codes. However, the resulting rate range is limited because the deletion of too many bits has a negative effect on decoding via belief propagation. To obtain a more dynamic range in rates, the technique of extending has been used. The extension is made by adding extra parity bits as illustrated in Fig. 3, where the overall code is the intersection of two constituent codes defined by H_2 and H_1 padded with zeros on the right.

For simplicity, we only used the technique of extending to acquire rate-compatibility, but this

may be further optimized by combining puncturing and extending via known techniques [14], [25], [41].

A. Full-diversity LDPC codes

Puncturing and erasing are slightly different in nature. From an algebraic decoding or a probabilistic decoding point of view, puncturing and erasing are identical, an erased/punctured bit is equivalent to an error with known location but unknown amplitude [26]. From a transmitter point of view, punctured bits have always fixed locations whereas channel erased bits have random locations. These similarities and differences in nature also exist for block erasures and block puncturing.

Full-diversity coding on a relay channel must cope with block erasures. Consider the coding structure plotted in Fig. 3. If all parity bits $2p$ are erased due to deep fading in frame 2, then the decoder should be capable to retrieve information bits i thanks to H_1 and possibly recompute $2p$ thanks to H_2 . Unfortunately, under deep fading in frame 1, a structure with a randomly generated H_2 as in Fig. 3, cannot guarantee the retrieval of the information bits through H_2 . The aim of this section is to explain how H_2 can be tuned in order to have full-diversity for

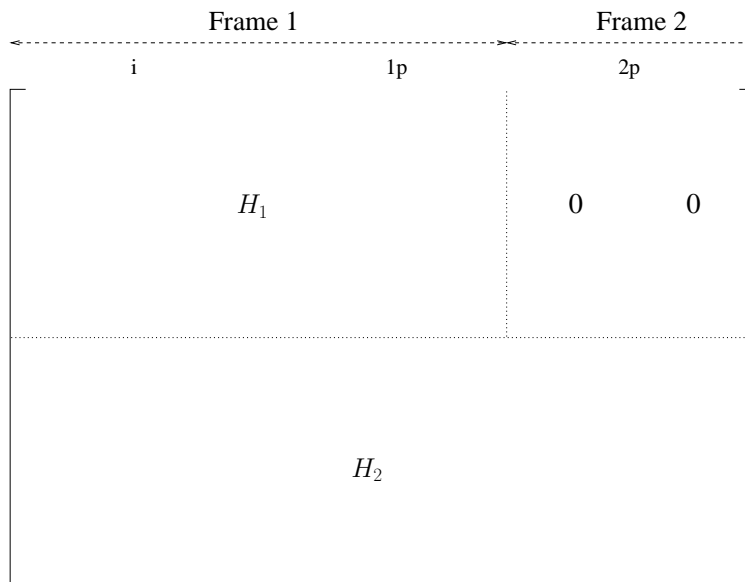


Fig. 3. Parity-Check matrix of a rate-compatible LDPC code obtained by the extension of higher rate codes. Symbols are split into three classes: i for the information bits, $1p$ and $2p$ for two classes of parity bits. The classes i and $1p$ are transmitted by the source in frame 1. Parity bits $2p$ are transmitted in the second frame, for example by the relay after successful decoding of the first frame.

any left and right degree distribution and for any block length. The cases 2 and 4 considered in Fig. 2 always have double diversity order or more for user 1, because at least two outage events are needed to lose the codeword, one on the source-destination channel and one on the interuser channel. Since case 3 has always a better performance than case 1 for user 1, we will assume in the following the occurrence of case 1 where the transmission on the interuser channel in the first frame has been successful and both users are cooperating in the second frame. This means that, for the transmission of user 1, the first fading state of the overall codeword is given by the user1-to-destination channel and the second fading state of the overall codeword is given by the user2-to-destination channel. The key to full-diversity codes will be to spread the information bits of a user over both frames.

Before describing the whole parity-check structure of a coded cooperation LDPC code in the next subsection, let us focus on the submatrix H_2 . We take the constituent code defined by H_2 to be a full-diversity LDPC code (referred to as root-LDPC code) as constructed by Boutros et al. in [9], [6] for non-cooperative single-antenna channels with two or more fading states per codeword. The Tanner graph notation for the root-LDPC code is given in Fig. 4. This notation is essential for the analysis because we seek full-diversity under iterative decoding. Full-diversity

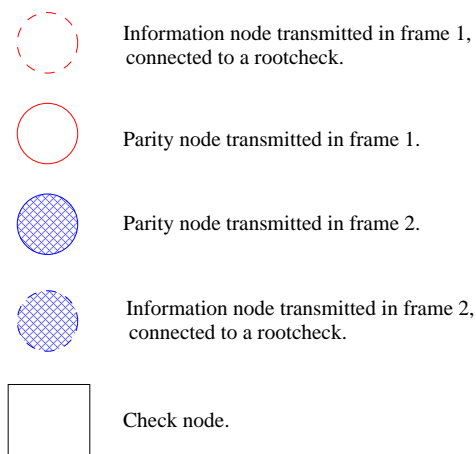


Fig. 4. Notation for the Tanner graph of a full-diversity LDPC code.

of a root-LDPC structure is created by *rootchecks*, a special type of checknodes in the Tanner graph. As shown in Fig. 5, the root and the leaves of this special checknode do not belong to the same frame. When the rootbit is in frame 1, the leavebits are in frame 2, and vice versa. Using

the limiting case of a Block-Erasure Channel, it is easy to verify that a rootbit is determined via its rootcheck when its own frame is erased. The complete root-LDPC structure is built after

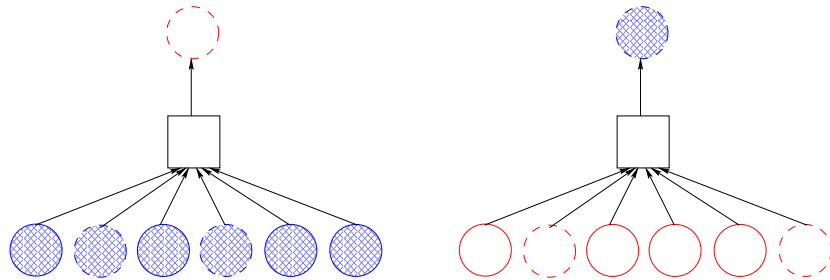


Fig. 5. Two types of rootchecks. On the left side, the rootbit belongs to frame 1 and the leafbits belong to frame 2. The symmetric case where channel states are switched is shown at the right side.

splitting information bits into two classes, denoted $1i$ and $2i$, and parity bits into two classes, denoted $1p$ and $2p$. The checknodes are cut into two classes denoted $3c$ and $4c$ ³. The classes $3c$ and $4c$ consist of rootchecks for information bits $1i$ and $2i$ respectively. The complete root-LDPC structure including all types of nodes is illustrated in Figs. 6 and 7. Rootchecks are translated into two identity matrices (or permutation matrices in general) inside the parity-check matrix in Fig. 7.

The proof of full-diversity for block-Rayleigh fading can be found in [9]. Note that the diversity order of the root-LDPC code does not depend on the right or left degree distributions. For simplicity, we only showed a regular (3,6) structure in Fig. 6.

For asymptotic code lengths, multiedge-type messages propagate in the root-LDPC graph [35]. One has to choose between two different root-LDPC ensembles. If we refer to the Tanner graph in Fig. 6, the two ensembles are distinguished as follows: (i) The first ensemble is built by two random edge permutations (edge interleavers) connecting $3c$ to $(2i, 2p)$ and $4c$ to $(1i, 1p)$ respectively. This is equivalent to the random generation of two low-density matrices (H_{2i}, H_{2p}) and (H_{1i}, H_{1p}) in the parity-check matrix shown in Fig. 7. (ii) The second ensemble is built by four random edge permutations $3c - 2i$, $3c - 2p$, $4c - 1i$, and $4c - 1p$. In the root-LDPC parity-check matrix, this is equivalent to building separately the four submatrices H_{2i} , H_{2p} , H_{1i} , and H_{1p} . For simplicity reasons, mainly in the density evolution (DE) analysis, we adopt the

³The checknode notation $1c$ and $2c$ is reserved for H_1 in the cooperative code as described in the next subsection.

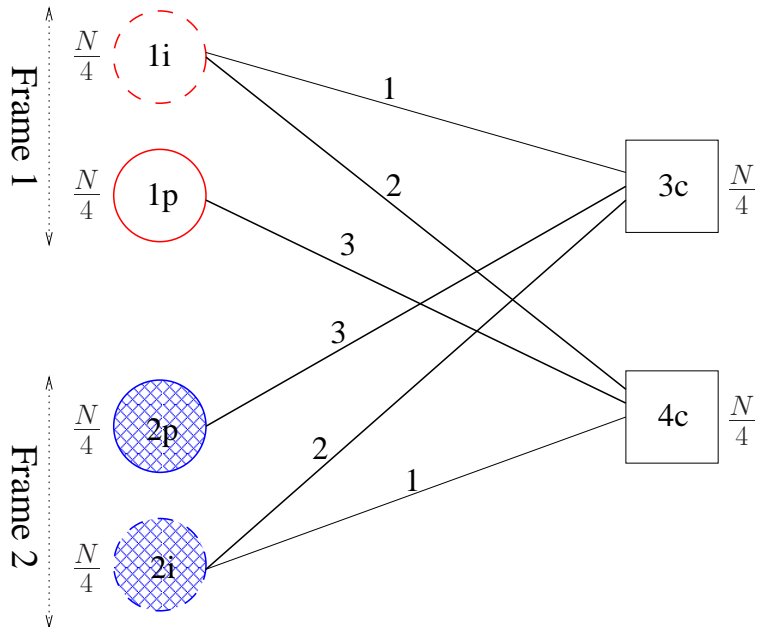


Fig. 6. Tanner graph of a full-diversity LDPC code of length N and rate $\frac{1}{2}$. This compact graph representation has been adopted from [9], [6], it is also known as protograph representation [38]. The integers labeling the edges of the Tanner graph indicate the degree of a node along those edges for a regular (3,6) root-LDPC code. The binary elements are split into four classes of each $\frac{N}{4}$ bits. The checknodes are cut into two classes of $\frac{N}{4}$ checks.

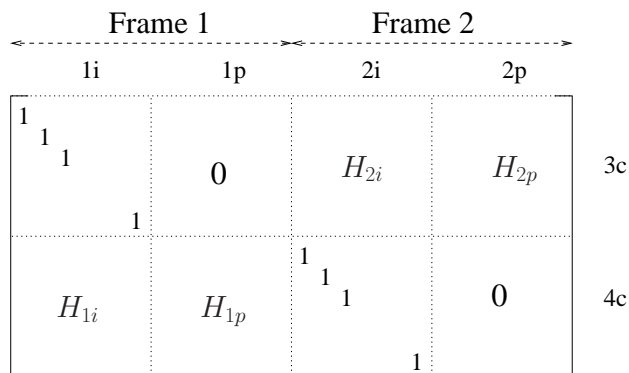


Fig. 7. Parity-Check matrix of a rate $\frac{1}{2}$ root-LDPC code.

first root-LDPC ensemble as part of the full-diversity cooperative code proposed in the next subsection.

B. Rate-compatible full-diversity LDPC codes

Now, the structure of a coded cooperation LDPC code is derived by joining the rate-compatibility property and the full-diversity property. In a first step, the global parity-check matrix is obtained

by embedding the root-LDPC matrix (Fig. 7) into the rate-compatible matrix (Fig. 3). This leads to an asymmetric code where class $1i$ may have a higher coding gain than class $2i$. In a second step, to get a balanced structure, we replace the zero-padded H_1 by the direct sum of two rate R_1 codes defined by H_{1s} and H_{1r} as illustrated in Fig. 8. Thus, the constituent code H_{1s} protects bits $1i$ and $1p$ via extra parity bits p'_1 . Similarly, in the second frame, extra parity bits p'_2 are generated from $2i$ and $2p$. The bottom of the global parity-check matrix simply includes the root-LDPC structure, connecting $(1i, 1p)$ to $(2i, 2p)$. For simplicity we can assume that H_{1s} and H_{1r} belong to the same random rate R_1 LDPC ensemble, defined by the degree distributions $(\lambda_1(x), \rho_1(x))$. Hence, if the degree distribution of the root-LDPC is $(\lambda_2(x), \rho_2(x))$, we refer to the rate-compatible root-LDPC as a $(\lambda_1(x), \rho_1(x), \lambda_2(x), \rho_2(x))$ code. The Tanner graphs of a regular $(3, 9, 3, 6)$ LDPC code and an irregular $(\lambda_1(x), \rho_1(x), \lambda_2(x), \rho_2(x))$ code are shown in Figs. 9 and 10. Since we guarantee full-diversity via a root-LDPC with a fixed rate $\frac{1}{2}$, the global coding rate of the rate-compatible root-LDPC code observed at the destination is $R_c = \frac{R_1}{2}$. As a consequence, the global coding rate R_c can be easily varied through R_1 .

Frame 1			Frame 2			
$1i$	$1p$	p'_1	$2i$	$2p$	p'_2	
H_{1s}			0	0	0	$1c$
0	0	0	H_{1r}			$2c$
1	1	1	0	0	0	$3c$
	1		H_{2i}	H_{2p}	0	
H_{1i}	H_{1p}	0	1	1	1	$4c$
				1		

Fig. 8. Parity-check matrix of a rate-compatible root-LDPC code for coded cooperation. The upper coding rate associated to H_{1s} and H_{1r} is $R_1 = \frac{2}{3}$, the bottom root-LDPC coding rate is $\frac{1}{2}$, and the overall coding rate is $R_c = \frac{R_1}{2} = \frac{1}{3}$.

Due to the identity matrices inside the parity-check matrix, new polynomials $\tilde{\lambda}_2(x)$ appear in Fig. 10 in the connections $1i - 4c$ and $2i - 3c$, as illustrated in Fig. 11.

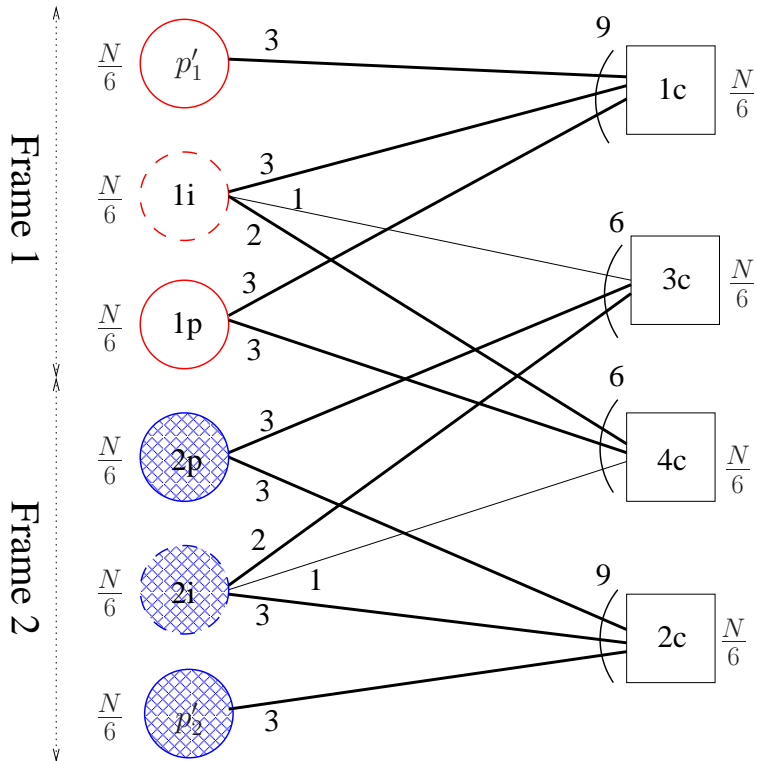


Fig. 9. Tanner graph of a regular $(3, 9, 3, 6)$ rate-compatible root-LDPC code for coded cooperation. We see that the average bit degree is $\bar{d}_b = 5$ and the average check degree is $\bar{d}_c = \frac{15}{2}$ which results in $R_c = 1 - \frac{\bar{d}_b}{\bar{d}_c} = \frac{1}{3}$.

Proposition 2 *In a Tanner graph with a left degree distribution $\lambda(x)$, isolating one edge per bitnode yields a new left degree distribution described by the polynomial $\tilde{\lambda}(x)$:*

$$\tilde{\lambda}(x) = \sum_i \tilde{\lambda}_i x^{i-1}, \quad \tilde{\lambda}_{i-1} = \frac{\lambda_i(i-1)/i}{\sum_j \lambda_j(j-1)/j}. \quad (10)$$

Proof: Let us define $T_{\text{bit},i}$ as the number of edges connected to a bitnode of degree i . Similarly, the number of all edges is denoted T_{bit} . From section II, we know that $\lambda(x) = \sum_{i=2}^{d_{b\max}} \lambda_i x^{i-1}$ expresses the left degree distribution, where λ_i is the fraction of all edges in the Tanner graph, connected to a bitnode of degree i . So finally $\lambda_i = \frac{T_{\text{bit},i}}{T_{\text{bit}}}$. A similar reasoning can

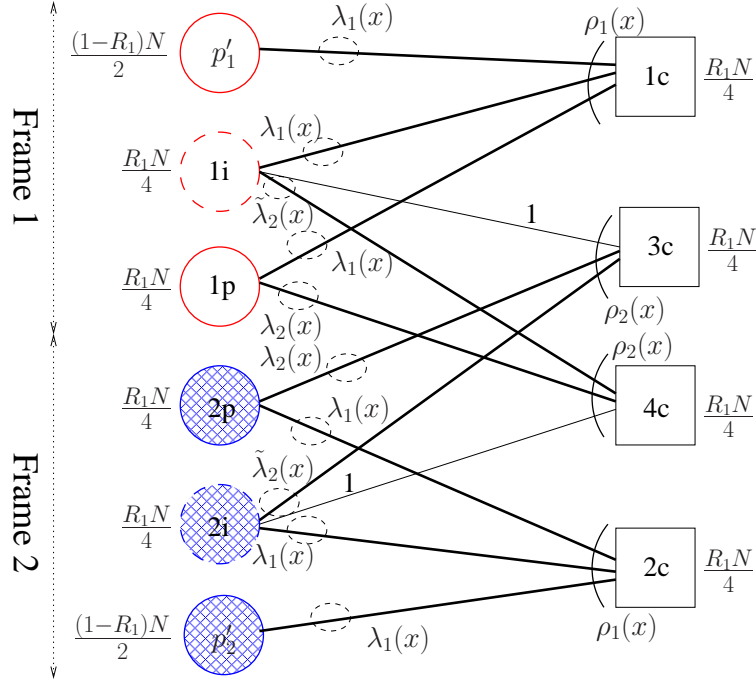


Fig. 10. Tanner graph of an irregular rate-compatible root-LDPC code for coded cooperation. The binary elements are split into six classes, p'_1 and p'_2 of each $\frac{(1-R_1)N}{2}$ bits and $1i$, $1p$, $2i$, and $2p$ of each $\frac{R_1N}{4}$ bits. The checknodes are cut into four classes of $\frac{R_1N}{4}$ checks.



Fig. 11. Transition from a traditional representation, characterized by an edge distribution polynomial $\lambda(x)$, towards a representation where one edge per bitnode is isolated resulting in a new degree distribution $\tilde{\lambda}(x)$.

be followed to determine $\tilde{\lambda}_i$:

$$\begin{aligned} \tilde{\lambda}_{i-1} &\stackrel{a)}{=} \frac{T_{\text{bit},i} - \frac{\lambda_i}{i} T_{\text{bit}}}{T_{\text{bit}} - \sum_j \frac{\lambda_j}{j} T_{\text{bit}}} \\ &\stackrel{b)}{=} \frac{\lambda_i T_{\text{bit}} - \frac{\lambda_i}{i} T_{\text{bit}}}{T_{\text{bit}} - \sum_j \frac{\lambda_j}{j} T_{\text{bit}}} \\ &= \frac{\lambda_i - \frac{\lambda_i}{i}}{\sum_j \frac{\lambda_j}{j} j - \sum_j \frac{\lambda_j}{j}} \\ &= \frac{\frac{\lambda_i}{i} (i-1)}{\sum_j \frac{\lambda_j}{j} (j-1)}. \end{aligned}$$

- a) $\sum_j \frac{\lambda_j}{j} T_{\text{bit}}$ is equal to the number of edges that are removed which is equal to the number of bits.
- b) $\lambda_i T_{\text{bit}}$ is equal to the number of edges connected to a bit of degree i .

■

In section V, we will also use $\tilde{\rho}(x)$, which is defined similarly as $\tilde{\lambda}(x)$.

Proposition 3 Consider a $(\lambda_1(x), \rho_1(x), \lambda_2(x), \rho_2(x))$ rate-compatible root-LDPC code for coded cooperation transmitted on a 2-user block-fading cooperative MAC. Then, under iterative belief propagation decoding, the rate-compatible root-LDPC code has full-diversity.

Proof: As indicated in the design of full-diversity LDPC codes in subsection IV-A, the diversity order of a root-LDPC code does not depend on its left or right degree distribution. Thus, we restrict this proof to a regular $(3, 9, 3, 6)$ LDPC code. Let Λ_i^a , $i = 1 \dots d_c - 1$ denote the input log-ratio probabilistic messages to a checknode Φ of degree d_c . The output message Λ^e for belief propagation is [33]

$$\Lambda^e = 2\text{th}^{-1} \left(\prod_{i=1}^{d_c-1} \text{th} \left(\frac{\Lambda_i^a}{2} \right) \right),$$

where $\text{th}(x)$ denotes the hyperbolic-tangent function. Superscripts a and e stand for *a priori* and *extrinsic*, respectively. To simplify the proof, we show that the suboptimal min-sum decoder yields a diversity order 2. For a min-sum decoder, the output message produced by a checknode Φ is now

$$\Lambda^e = \min(|\Lambda_i^a|) \prod_{i=1}^{d_c-1} \text{sign}(\Lambda_i^a).$$

An information bit ϑ of class $1i$ has $\Lambda_0 = \frac{2\alpha_1 y_{sr}}{\sigma^2}$ where Λ_0 is the log-likelihood ratio coming from the likelihood $p(y_{sr}|\vartheta)$. It also receives 6 messages Λ_{ij}^e , $i = 1 \dots 3$ for its three neighbouring checknodes in each constituent code, $j = 1, 2$ for the 2 constituent codes H_{1s} and H_2 respectively. The total *a posteriori* message corresponding to ϑ is $\Lambda = \Lambda_0 + \sum_{j=1}^2 \sum_{i=1}^3 \Lambda_{ij}^e$. The addition of $\sum_{i=1}^3 \Lambda_{i1}^e$ cannot degrade the error probability $P_e(1i)$ because the convolution with the density of messages from H_{1s} can only physically upgrade the resulting density. Thus, it is sufficient to prove that message $\Lambda_0 + \sum_{i=1}^3 \Lambda_{i2}^e$ exhibits full-diversity, which is proven in [9]. ■

V. DENSITY EVOLUTION ON THE BLOCK-FADING RELAY CHANNEL

Richardson and Urbanke [32], [33] established that, if the block length is large enough, (almost) all codes in an ensemble of codes⁴ behave alike, so the determination of the average behavior is sufficient to characterize a particular code behavior. This average behavior converges to the cycle-free case if the block length augments and it can be found in a deterministic way through density evolution (DE). The evolution trees represent the local neighborhood of a bitnode in an infinite length code whose graph has no cycles, hence incoming messages to every node are independent.

A. Interuser channel

To determine the density of messages propagating in the graph of the constituent code $H_{1,s}$, the following notation is used:

$$d_{sr}^m(x) = \text{density of message from a bitnode to a checknode in the } m^{\text{th}} \text{ iteration.} \quad (11)$$

$$\mu_{sr}(x) = \text{density of the likelihood of the source-relay channel.} \quad (12)$$

Let $X_1 \sim p_1(x)$ and $X_2 \sim p_2(x)$ be two independent real random variables. The density function of $X_1 + X_2$ is obtained by convolving the two original densities, written as $p_1(x) \otimes p_2(x)$. The notation $p(x)^{\otimes n}$ denotes the convolution of $p(x)$ with itself n times.

Let $X_1 \sim p_1(x)$ and $X_2 \sim p_2(x)$ be two independent real random variables. The density function $p(y)$ of the variable $Y = 2 \operatorname{th}^{-1} \left(\operatorname{th} \left(\frac{X_1}{2} \right) \operatorname{th} \left(\frac{X_2}{2} \right) \right)$, obtained through a checknode with X_1 and X_2 at the input, is obtained through the *R-convolution* [33], written as $p_1(x) \odot p_2(x)$. The notation $p(x)^{\odot n}$ denotes the R-convolution of $p(x)$ with itself n times.

To simplify the notations, we use the following definitions:

⁴The ensemble of all LDPC-codes that satisfy the left degree distribution $\lambda(x)$ and right degree distribution $\rho(x)$ is considered. The ensemble is equipped with a uniform probability distribution.

$$\lambda(p(x)) = \sum_i \lambda_i p(x)^{\otimes i-1}, \quad \rho(p(x)) = \sum_i \rho_i p(x)^{\odot i-1}.$$

In the next subsection we will also use the following definitions:

$$\begin{aligned} \rho(p(x), t(x)) &= \sum_i (\rho_i p(x)^{\odot i-1} \odot t(x)), \\ \lambda^*(p(x)) &= \lambda(p(x)) \otimes (p(x)), \quad \rho^*(p(x)) = \rho(p(x)) \odot (p(x)). \end{aligned}$$

The first definition is necessary because of the non-linearity of the R-convolution. Therefore, the first equation is not equal to $t(x) \odot \rho(p(x))$. The next subsection will also use the polynomials $\dot{\rho}^*(x)$ and $\dot{\lambda}^*(x)$ which are defined by combining the two transformations, denoted by $\dot{(\cdot)}$ (see introduction) and $(\cdot)^*$.

Fig. 12 illustrates the local neighborhood of a bitnode in the constituent code H_{1s} .

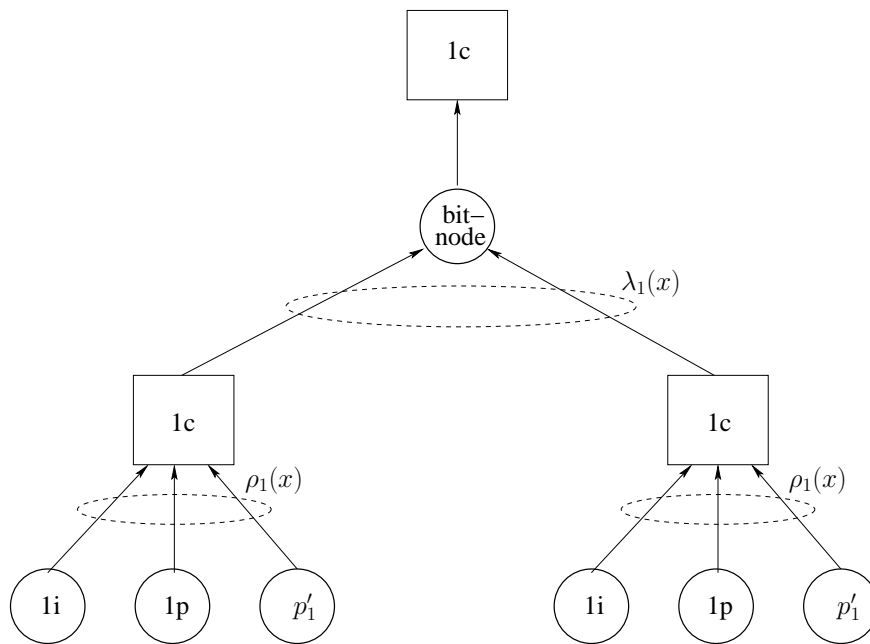


Fig. 12. Local neighborhood of a bitnode in the constituent code H_{1s} . This tree is used to determine the evolution of density $d_{sr}(x)$ of messages from a bitnode to a checknode.

The DE equation in the neighborhood of the bitnode for a $(\lambda_1(x), \rho_1(x))$ LDPC code [32] is,

for all m ,

$$d_{sr}^{m+1}(x) = \mu_{sr}(x) \otimes \lambda_1 \left(\rho_1(d_{sr}^m(x)) \right). \quad (13)$$

The threshold of a code is the minimum SNR at which a codeword can be decoded perfectly [32]. Comparing the received signal-to-noise ratio with this threshold, the relay and the source can determine whether the interuser transmissions can be decoded successfully and consequently decide what to transmit in the second frame.

B. Overall two-user MAC

The proposed $(\lambda_1(x), \rho_1(x), \lambda_2(x), \rho_2(x))$ root-LDPC code has 6 variable node types and 4 checknode types. Consequently, the evolution of message densities under iterative decoding has to be described through multiple evolution trees for a binary root-LDPC code. Figs. 13, 15, 16, 17, 18, and 19 show the local neighborhood of classes $1i$, $1p$, and p'_1 . The local neighborhood of classes $2i$, $2p$, and p'_2 are equivalent because of code symmetry.

To determine the density of messages, the following notation is used:

$$\begin{aligned} a_1^m(x), a_2^m(x) &= \text{density of message from } 1i \text{ to } 1c \text{ and } 2i \text{ to } 2c \text{ respectively, at the } m^{\text{th}} \text{ iteration,} \\ f_1^m(x), f_2^m(x) &= \text{density of message from } 1i \text{ to } 3c \text{ and } 2i \text{ to } 4c \text{ respectively, at the } m^{\text{th}} \text{ iteration,} \\ g_1^m(x), g_2^m(x) &= \text{density of message from } 1i \text{ to } 4c \text{ and } 2i \text{ to } 3c \text{ respectively, at the } m^{\text{th}} \text{ iteration,} \\ k_1^m(x), k_2^m(x) &= \text{density of message from } 1p \text{ to } 1c \text{ and } 2p \text{ to } 2c \text{ respectively, at the } m^{\text{th}} \text{ iteration,} \\ l_1^m(x), l_2^m(x) &= \text{density of message from } 1p \text{ to } 4c \text{ and } 2p \text{ to } 3c \text{ respectively, at the } m^{\text{th}} \text{ iteration,} \\ q_1^m(x), q_2^m(x) &= \text{density of message from } p'_1 \text{ to } 1c \text{ and } p'_2 \text{ to } 2c \text{ respectively in the } m^{\text{th}} \text{ iteration,} \\ \mu_i(x) &= \text{density of the likelihood of the channel in the } i^{\text{th}} \text{ frame.} \end{aligned}$$

Note that $\mu_2(x)$ depends on the success or the failure of the transmissions in the first frame.

In Figs. 13, 15, 16, the local neighborhood of a bitnode of the class $1i$ is given.

Proposition 4 *The DE equations in the neighborhood of $1i$, $1p$ and p'_1 for a $(\lambda_1(x), \rho_1(x), \lambda_2(x), \rho_2(x))$*

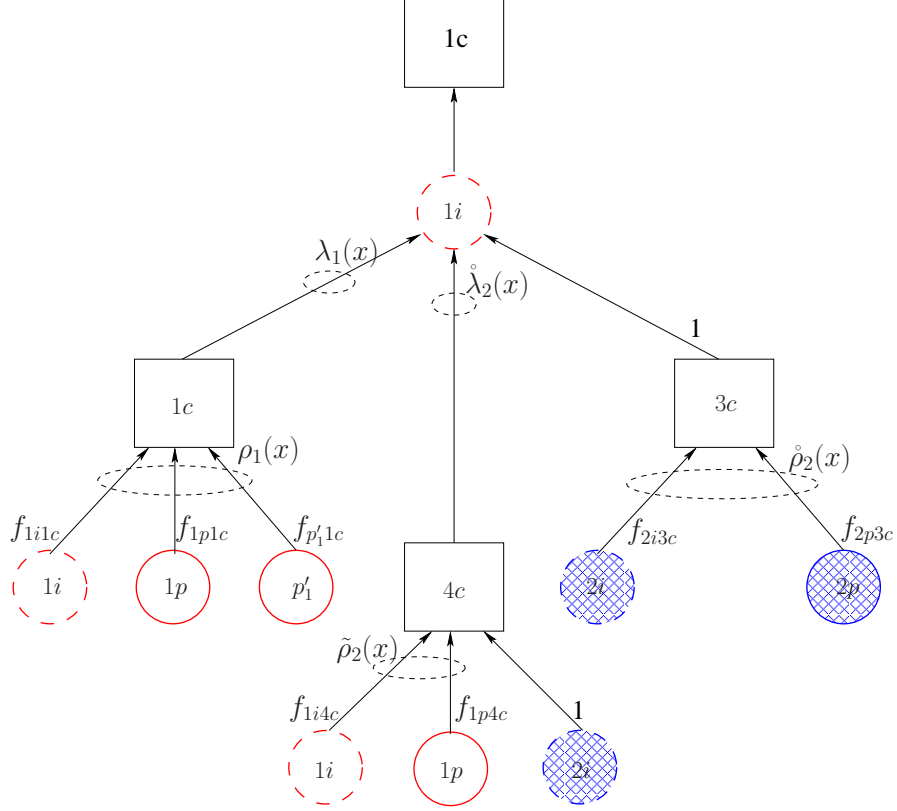


Fig. 13. Local neighborhood of bitnode $1i$. This tree is used to determine the evolution of the density of messages $1i \rightarrow 1c$.

root-LDPC code for coded cooperation are, for all m ,

$$\begin{aligned}
 a_1^{m+1}(x) &= \mu_1(x) \otimes \dot{\lambda}_2 \left(\tilde{\rho}_2(f_{1i4c} g_1^m(x) + f_{1p4c} l_1^m(x), f_2^m(x)) \right) \\
 &\quad \otimes \lambda_1 \left(\rho_1(f_{1i1c} a_1^m(x) + f_{1p1c} k_1^m(x) + f_{p'1c} q_1^m(x)) \right) \\
 &\quad \otimes \dot{\rho}_2 \left(f_{2i3c} g_2^m(x) + f_{2p3c} l_2^m(x) \right), \tag{14}
 \end{aligned}$$

$$\begin{aligned}
 f_1^{m+1}(x) &= \mu_1(x) \otimes \dot{\lambda}_1^* \left(\rho_1(f_{1i1c} a_1^m(x) + f_{1p1c} k_1^m(x) + f_{p'1c} q_1^m(x)) \right) \\
 &\quad \otimes \dot{\lambda}_2 \left(\tilde{\rho}_2(f_{1i4c} g_1^m(x) + f_{1p4c} l_1^m(x), f_2^m(x)) \right), \tag{15}
 \end{aligned}$$

$$\begin{aligned}
g_1^{m+1}(x) &= \mu_1(x) \otimes \dot{\lambda}_1^* \left(\rho_1 (f_{1i1c} a_1^m(x) + f_{1p1c} k_1^m(x) + f_{p'1c} q_1^m(x)) \right) \\
&\quad \otimes \tilde{\lambda}_2 \left(\tilde{\rho}_2 (f_{1i4c} g_1^m(x) + f_{1p4c} l_1^m(x), f_2^m(x)) \right) \\
&\quad \otimes \dot{\rho}_2 \left(f_{2i3c} g_2^m(x) + f_{2p3c} l_2^m(x) \right), \tag{16}
\end{aligned}$$

$$\begin{aligned}
k_1^{m+1}(x) &= \mu_1(x) \otimes \dot{\lambda}_2^* \left(\tilde{\rho}_2 (f_{1i4c} g_1^m(x) + f_{1p4c} l_1^m(x), f_2^m(x)) \right) \\
&\quad \otimes \lambda_1 \left(\rho_1 (f_{1i1c} a_1^m(x) + f_{1p1c} k_1^m(x) + f_{p'1c} q_1^m(x)) \right), \tag{17}
\end{aligned}$$

$$\begin{aligned}
l_1^{m+1}(x) &= \mu_1(x) \otimes \dot{\lambda}_1^* \left(\rho_1 (f_{1i1c} a_1^m(x) + f_{1p1c} k_1^m(x) + f_{p'1c} q_1^m(x)) \right) \\
&\quad \otimes \lambda_2 \left(\tilde{\rho}_2 (f_{1i4c} g_1^m(x) + f_{1p4c} l_1^m(x), f_2^m(x)) \right), \tag{18}
\end{aligned}$$

$$q_1^{m+1}(x) = \mu_1(x) \otimes \lambda_1 \left(\rho_1 (f_{1i1c} a_1^m(x) + f_{1p1c} k_1^m(x) + f_{p'1c} q_1^m(x)) \right) \tag{19}$$

where

$$f_{1p4c} = \frac{\sum_i \tilde{\rho}_{2i}/i}{\sum_i \lambda_{2i}/i}, \tag{20}$$

$$f_{1i4c} = \frac{\sum_i \tilde{\rho}_{2i}/i}{\sum_i \tilde{\lambda}_{2i}/i}, \tag{21}$$

$$f_{1p1c} = \frac{\sum_i \rho_{1i}/i}{\sum_i \lambda_{1i}/i}, \tag{22}$$

$$f_{1i1c} = f_{1p1c}, \tag{23}$$

$$f_{p'1c} = 1 - f_{1i1c} - f_{1p1c}, \tag{24}$$

$$f_{2i3c} = f_{1i4c}, \tag{25}$$

$$f_{2p3c} = f_{1p4c}. \tag{26}$$

Proof: Equations (14)-(26) are directly derived from the local neighborhood trees. To obtain the proportionality factors (20)-(26), it is important to remark that we use the first ensemble of root-LDPC codes, as explained at the end of section IV-A. Let T denote the total number of edges between the variable nodes $(1i - 1p)$ and the checknodes $4c$. Fig. 14 illustrates how f_{1p4c} and f_{1i4c} are obtained:

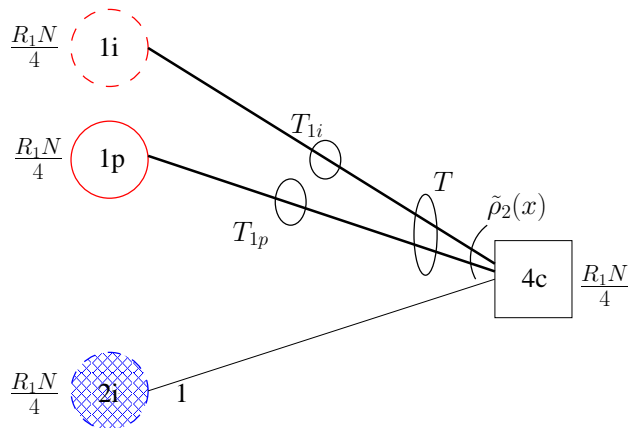


Fig. 14. Part of the compact graph representation of the Tanner graph of a root-LDPC for coded cooperation. The number of edges connecting $(1i, 1p)$ to $4c$ is T , the number of edges connecting $1p$ to $4c$ is T_{1p} . The number of edges connecting $1i$ to $4c$ is T_{1i} .

$$T \stackrel{a)}{=} \frac{R_1 N/4}{\sum_i \tilde{\rho}_{2i}/i} \quad (27)$$

$$T_{1p} \stackrel{a)}{=} \frac{R_1 N/4}{\sum_i \lambda_i/i} \quad (28)$$

$$T_{1i} \stackrel{a)}{=} \frac{R_1 N/4}{\sum_i \tilde{\lambda}_i/i} \quad (29)$$

$$f_{1p4c} \stackrel{b)}{=} \frac{T_{1p}}{T} \quad (30)$$

$$f_{1i4c} \stackrel{b)}{=} \frac{T_{1i}}{T}. \quad (31)$$

- a) The number of checknodes connected to i edges of T is $\frac{\tilde{\rho}_{2i}}{i}T$. A Similar reasoning proves equations (28) and (29).
- b) The fraction of edges T connecting $1p$ to $4c$ is f_{1p4c} . The fraction of edges T connecting $1i$ to $4c$ is f_{1i4c} .

■

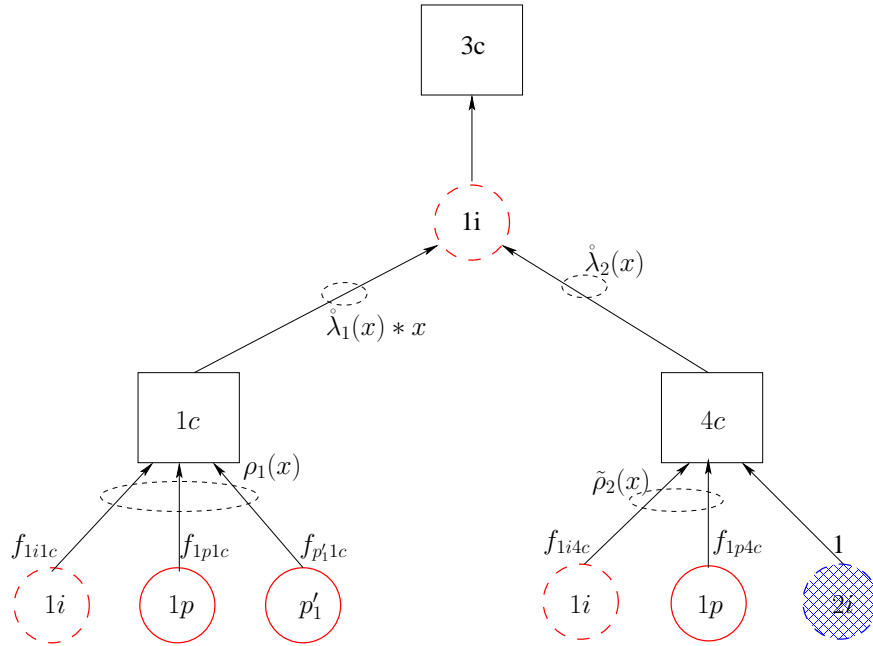


Fig. 15. Local neighborhood of bitnode $1i$. This tree is used to determine the evolution of the density of messages $1i \rightarrow 3c$.

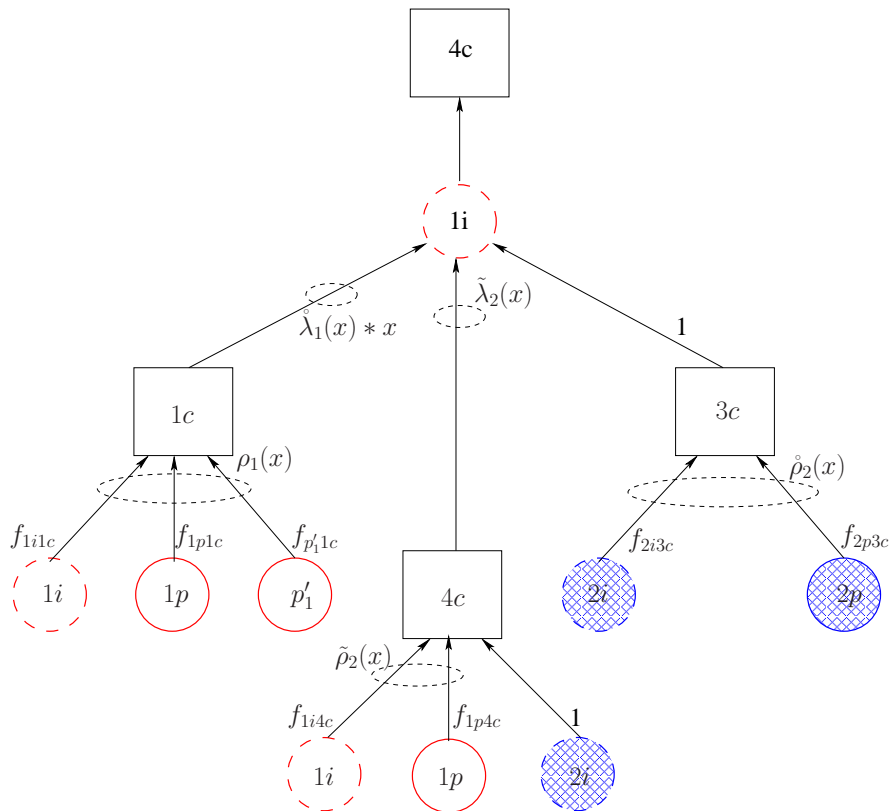


Fig. 16. Local neighborhood of bitnode $1i$. This tree is used to determine the evolution of the density of messages $1i \rightarrow 4c$.

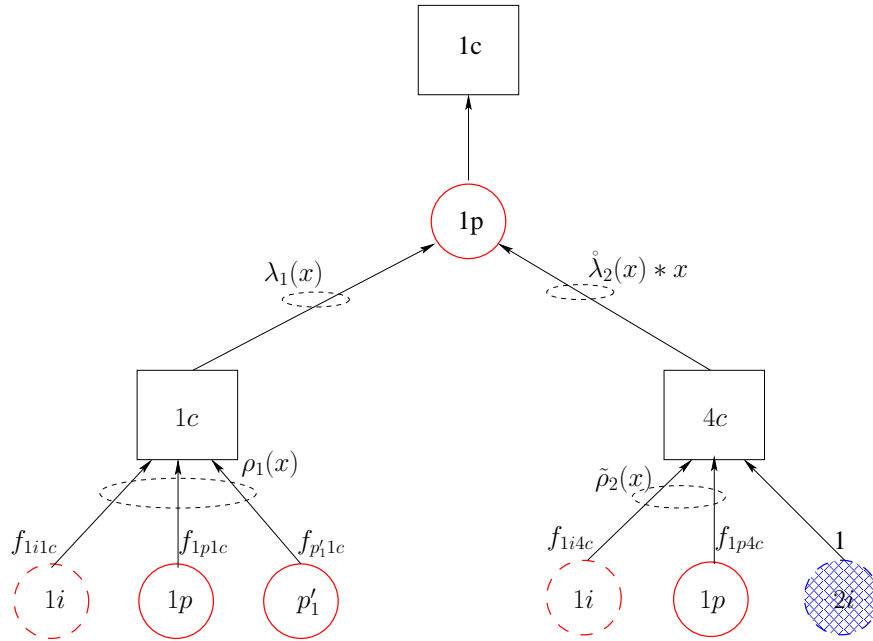


Fig. 17. Local neighborhood of bitnode $1p$. This tree is used to determine the evolution of the density of messages $1p \rightarrow 1c$.

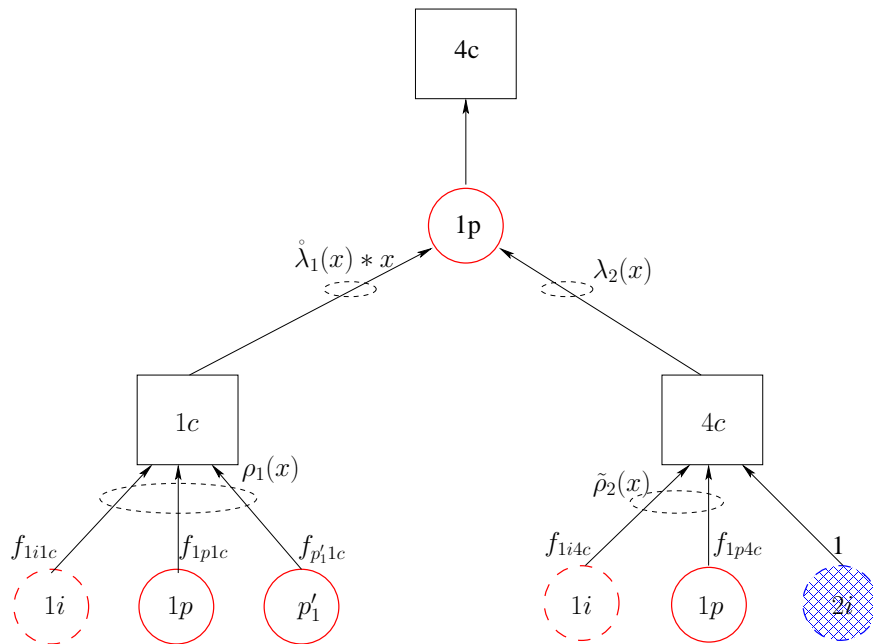


Fig. 18. Local neighborhood of bitnode $1p$. This tree is used to determine the evolution of the density of messages $1p \rightarrow 4c$.

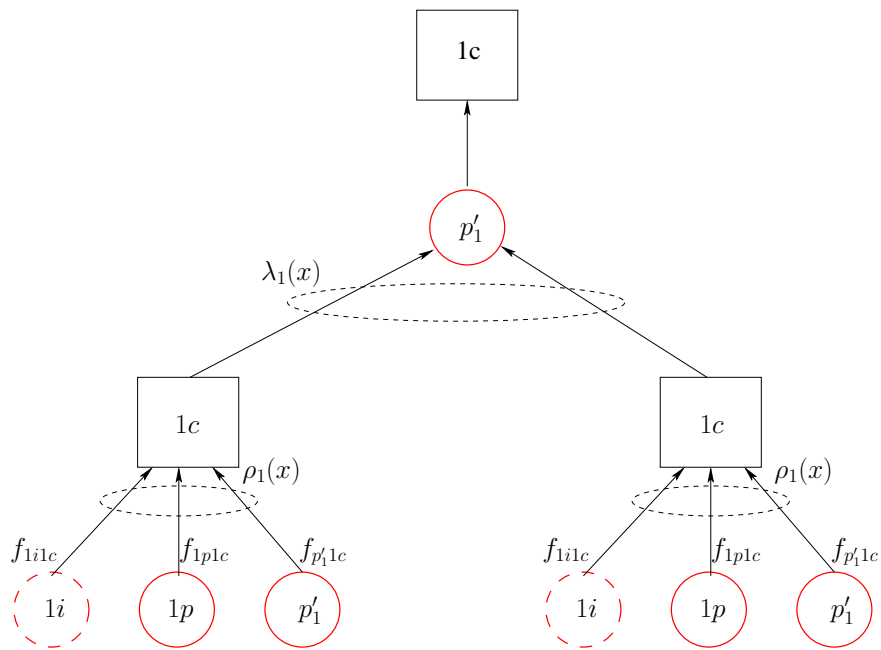


Fig. 19. Local neighborhood of bitnode p'_1 . This tree is used to determine the evolution of the density of messages $p'_1 \rightarrow 1c$.

VI. NUMERICAL RESULTS

A. Infinite Length Codes

We evaluated the asymptotic performance of rate-compatible root-LDPC codes by applying DE on the proposed code construction. We studied different scenarios:

1) Scenario 1:

- The average SNR of the independent interuser channels is 5dB higher than the average SNR on the source-destination link.
- The average SNR of the relay-destination link is equal to that on the source-destination link.
- The coding rate is $R_c = \frac{1}{3}$ and the cooperation level is $\beta = 0.5$.

Fig. 20 shows the main results: the word error rate (WER) of a regular (3,9,3,6) rate-compatible root-LDPC code and of an irregular $(\lambda_1(x), \rho_1(x), \lambda_2(x), \rho_2(x))$ rate-compatible root-LDPC code with left and right degree distributions given by the polynomials

$$\lambda_1(x) = 0.1989x + 0.2305x^2 + 0.0068x^5 + 0.2774x^6 + 0.14267x^{19} + 0.1335x^{20} + 0.0102x^{21},$$

$$\rho_1(x) = x^{12},$$

$$\lambda_2(x) = 0.22767x + 0.20333x^2 + 0.2145x^5 + 0.011048x^6 + 0.34346x^{19},$$

$$\rho_2(x) = 0.5x^7 + 0.5x^8.$$

As can be seen clearly on the figure, the regular rate-compatible root-LDPC code is always within 1.5dB from the outage probability limit, whereas the irregular rate-compatible root-LDPC code is always within 1dB from the outage probability limit. This distance is respected for many variations of the channel conditions, such as other interuser channel conditions or uplink channel conditions. Note that our code construction can, just as in [16], be applied on a full-duplex channel, doubling the overall spectral efficiency. As mentioned before, the coding rate is adjustable by varying the number of parity bits p'_1 and p'_2 , which is illustrated in scenario 2.

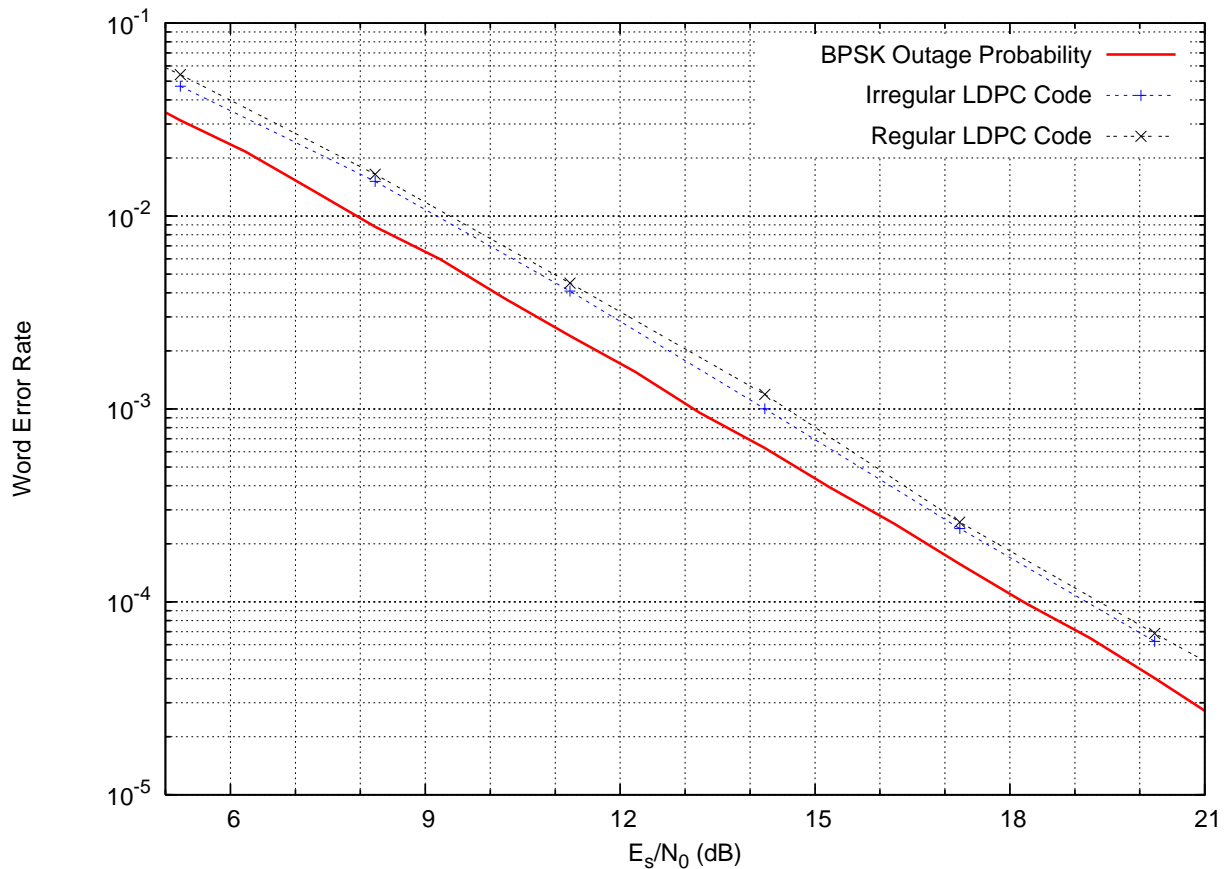


Fig. 20. Density evolution of rate-compatible root-LDPC codes with coding rate $R_c = \frac{1}{3}$ with iterative decoding on a cooperative MAC with two users. E_s/N_0 is the average symbol energy-to-noise ratio on the source-destination link.

2) Scenario 2:

- The average SNR of the independent interuser channels is 12dB higher than the average SNR on the source-destination link.
- The average SNR of the relay-destination link is 4dB higher than the average SNR on the source-destination link.
- The coding rate is $R_c = 0.45$ and the cooperation level is $\beta = 0.5$.

Here, we imitated the channel conditions used in [16]. These channel conditions are optimistic, allowing a high coding-rate for the source-relay channel. Fig. 21 illustrates the WER of an irregular $(\lambda_1(x), \rho_1(x), \lambda_2(x), \rho_2(x))$ rate-compatible root-LDPC code with left and right degree

distributions given by the polynomials

$$\lambda_1(x) = 0.1581x + 0.2648x^2 + 0.1116x^5 + 0.1354x^6 + 0.3301x^{14},$$

$$\rho_1(x) = x^{43},$$

$$\lambda_2(x) = 0.234413x + 0.21392x^2 + 0.123711x^5 + 0.125548x^6 + 0.30241x^{19},$$

$$\rho_2(x) = 0.71875x^7 + 0.28125x^8.$$

The coding rate for the interuser channel subcode H_1 is equal to 0.9.

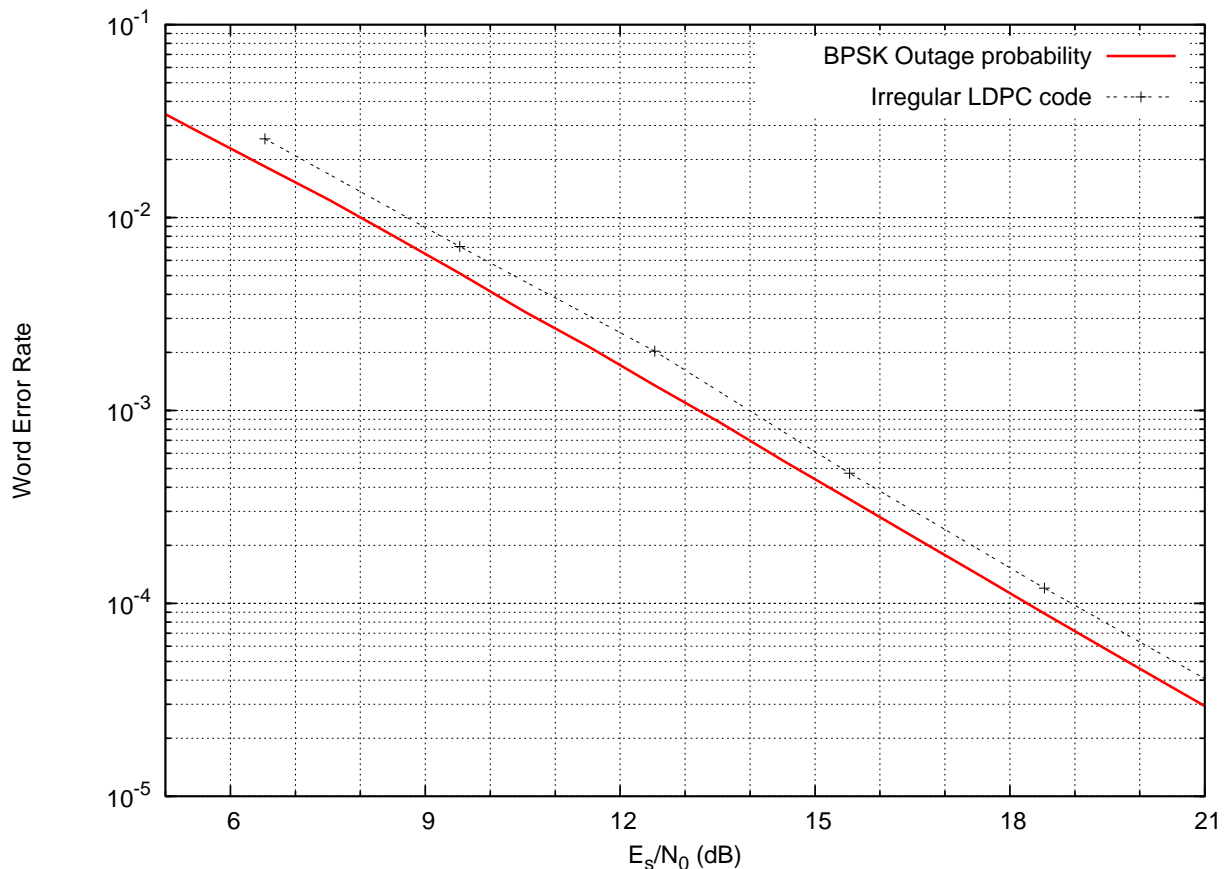


Fig. 21. Density evolution of rate-compatible root-LDPC codes with coding rate $R_c = 0.45$ with iterative decoding on a cooperative MAC with two users. E_s/N_0 is the average symbol energy-to-noise ratio on the source-destination link.

Fig. 21 shows that a rate-compatible root-LDPC code with a coding rate approaching $\frac{1}{2}$ still exhibits a near-outage performance. A code is referred to as MDS code [20], [27] when the diversity order is equal to $\lfloor N_u(1 - R_c) \rfloor + 1$, where N_u is the number of users. In contrast to code constructions previously published in the literature where no root-LDPC codes are used,

this code construction renders an MDS code (the diversity order is still two if a coding rate $R_c = 0.5$ is adopted), because the diversity order only depends on the constituent code H_2 , which has been shown to be MDS in [9]. However, it is not possible to show DE results for the rate-compatible root-LDPC with a coding rate $R_c = 0.5$, because this implies that $R_1 = 1$ and that there is no threshold effect on the interuser channel.

B. Finite Length LDPC Codes

It is interesting to evaluate the finite length performance of the proposed rate-compatible root-LDPC codes. Not only to approve the asymptotic performance, but also to see how to generate an instance of the parity-check matrix, given by Fig. 8. Before showing the results, we will first discuss the practical generation of this parity-check matrix.

Consider case 1 from Fig. 2. For the decoding process, the destination will apply the sum-product algorithm on the overall graph including H_{1s} , H_{1r} , and H_2 . For the encoding process, it is easier to determine the parity bits p'_1 , p'_2 , and $(1p, 2p)$ with the parity-check matrices H_{1s} , H_{1r} , and H_2 respectively. As with standard LDPC encoding, these matrices will then be systemized to determine the parity bits. An important constraint for the decoding process is the alignment in the overall parity-check matrix of common bit nodes in both constituent codes. This can be achieved by prohibiting column permutations during the systemization of H_{1s} , H_{1r} and H_2 . Except for case 4, which only decodes on H_{1s} , the other cases need the same constraints.

1) *Generation of H_{1s} and H_{1r} :* H_{1s} and H_{1r} are randomly generated satisfying the degree distribution $\rho_1(x)$ for its rows and the degree distribution $\lambda_1(x)$ for its columns. A sufficient condition to prohibit column permutations during the systemization of H_{1s} and H_{1r} is imposing on $H_{p'_1}$ and $H_{p'_2}$ to be full-rank. $H_{p'_1}$ ($H_{p'_2}$ respectively) is the most right square matrix of H_{1s} (H_{1r} respectively).

2) *Generation of H_2 :* The generation of H_2 can be split in the generation of H_{4c} and H_{3c} , where H_{3c} (H_{4c} resp.) is the upper part (resp. lower part) of the parity-check matrix H_2 . H_{3c} is the concatenation of an identity matrix (permutation matrix), zeros and a randomly generated matrix (H_{2i}, H_{2p}) . The rows of (H_{2i}, H_{2p}) satisfy the degree distribution $\tilde{\rho}_2(x)$, the columns of the most left square matrix H_{2i} satisfy the degree distribution $\tilde{\lambda}_2(x)$ and the columns of the most

right square matrix H_{2p} satisfy the degree distribution $\lambda_2(x)$. This is equivalent to generating a random graph with two classes of bitnodes at the left side and one class of checknodes at the right side of the graph. If n_{3c} is the number of checknodes at the right side, then a random graph with $\frac{n_{3c}}{\sum_i \tilde{\rho}_{2i}}$ edges is generated. A fraction $\frac{\sum_i \tilde{\rho}_{2i}/i}{\sum_i \tilde{\lambda}_{2i}/i}$ of the edges is connected to bit nodes of the class $2i$, whereas a fraction $\frac{\sum_i \tilde{\rho}_{2i}/i}{\sum_i \tilde{\lambda}_{2i}/i}$ of the edges is connected to bit nodes of the class $2p$. In the end, the identity matrix is simply added. H_{4c} is generated similarly.

For the encoding process, we have to systemize this matrix. One solution is to switch the columns associated with the $1i$ bit node class and the $2p$ bit node class. The most left square matrix of H_2 will then be block-diagonal with H_{2p} and H_{1p} on its diagonal. Having H_{2p} and H_{1p} full-rank is consequently a sufficient condition to exclude column permutations during the systemization of this matrix. After the generation of $(2p, 1p)$, all the bits are put in the required order $1i - 1p - 2i - 2p$ by switching back the bits of the classes $1i$ and $1p$.

3) *WER performance of finite length LDPC codes:* The WER performance of different block lengths is illustrated by Fig. 22. We used the same channel conditions and coding rate as in scenario 1 in the previous subsection. This figure approves the DE results for an asymptotic block length.

C. Comparison with previous work

As mentioned in the introduction, especially rate-compatible punctured convolutional codes (RCPC) have been used in coded cooperation. The main drawback of these codes is that the WER increases with the logarithm of the block length to the power d where d is the diversity order [7], [8], whereas the WER of near-outage codes should be independent of the block length. This can be seen clearly on Fig. 23, where we show the WER of two rate-compatible non-recursive non-systematic (75,53,47) convolutional codes with blocklength 500 and 5000 respectively. We used the same channel conditions and coding rate as in scenario 1 in subsection VI-A.

We also compared with another protocol, Decode and Forward (DF), using near-outage LDPC codes for this protocol. Despite the fact that this implementation has near-outage performance, the WER performance is worse than that of our code construction. The reason is that the outage probability limit of DF is higher than that of coded cooperation.

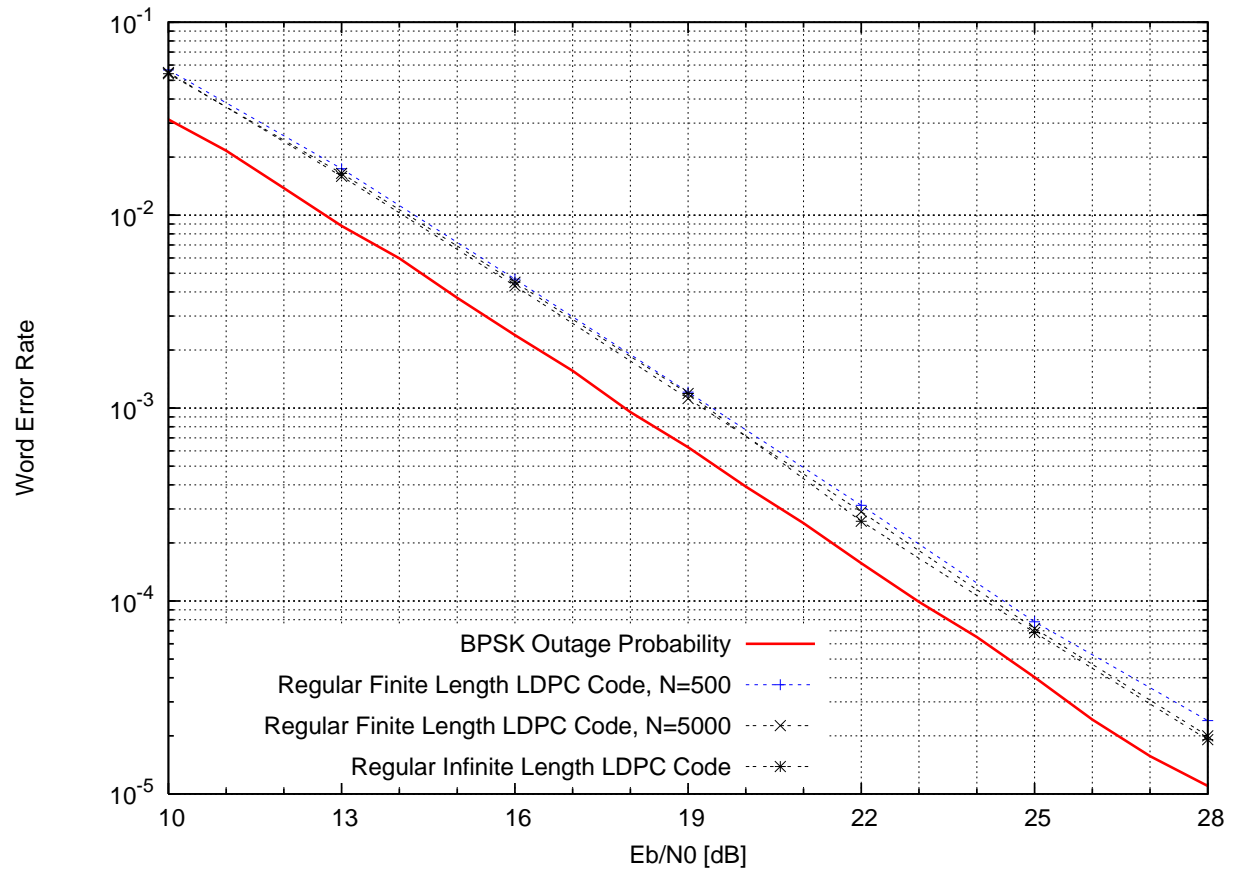


Fig. 22. Comparison of rate-compatible root-LDPC codes for different block lengths with iterative decoding on a cooperative MAC for two users, coding rate $R_c = 1/3$. The ratio E_b/N_0 is the average information bit energy-to-noise ratio on the source-destination link.

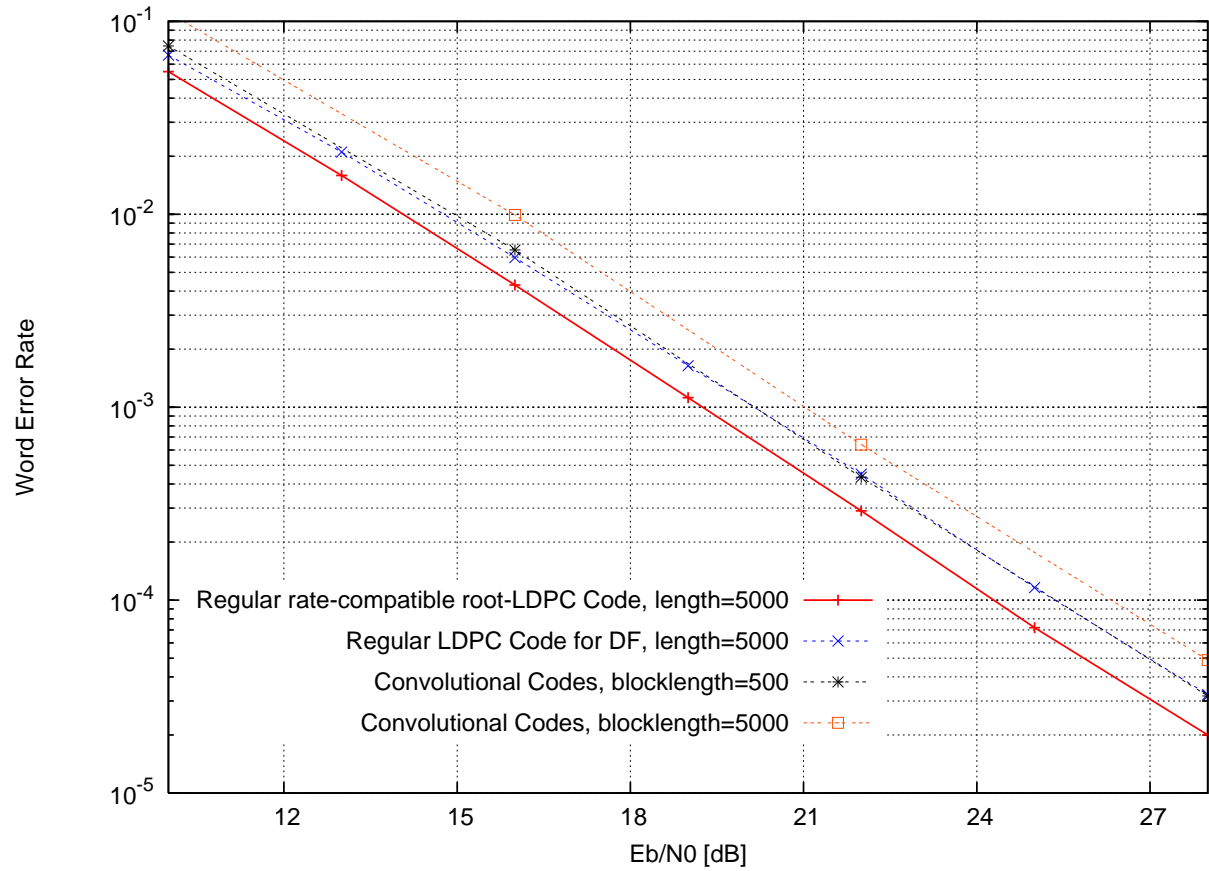


Fig. 23. Comparison of rate-compatible root-LDPC codes for coded cooperation with other work on a cooperative MAC for two users. We simulated LDPC codes for Decode and Forward under iterative decoding and an implementation of rate-compatible convolutional codes [17]. The ratio E_b/N_0 is the average information bit energy-to-noise ratio on the source-destination link.

VII. CONCLUSION

We have studied LDPC codes for relay channels in a slowly varying fading environment under iterative decoding. We have introduced the new family of rate-compatible root-LDPC codes, which combines the rate-compatibility property with the full-diversity property for any coding rate $R_c \leq R_{cmax} = \min(\beta, 1 - \beta)$, where β is the cooperation level. We have shown that the error rate performance of regular and irregular rate-compatible root-LDPC codes is close to the outage probability limit and this occurs for all block lengths (finite and infinite) and all rates not exceeding R_{cmax} . Its flexibility and high performance makes rate-compatible root-LDPC attractive for wireless cooperative communications scenarios with slowly varying fading.

REFERENCES

- [1] K. Azarian, H. El Gamal, and P. Schniter, "On the achievable diversity-multiplexing tradeoff in half-duplex cooperative channels," *IEEE Trans. on Inf. Theory*, vol. 51, no. 12, pp. 4152-4172, Dec. 2005.
- [2] X. Bao and J. Li, "Decode-amplify-forward (DAF): a new class of forwarding strategy for wireless relay channels," *Proc. IEEE SPAWC*, New York, pp. 816-820, June 2005.
- [3] C. Berrou, A. Glavieux, and P. Thitimajshima, "Near Shannon limit error-correcting coding and decoding: Turbo-codes," *ICC '93*, Conference Record, Geneva, pp.1064-1070, May 1993.
- [4] E. Biglieri, J. Proakis, S. Shamai, "Fading channels: information-theoretic and communications aspects," *IEEE Trans. on Inf. Theory*, vol. 44, no. 6, pp. 2619-2692, Oct. 1998.
- [5] E. Biglieri, *Coding for wireless channels*, Springer, 2005.
- [6] J.J. Boutros, A. Guillén i Fàbregas, E. Biglieri, and G. Zémor, "Design and Analysis of Low-Density Parity-Check Codes for Block-Fading Channels," *Information Theory and Applications Workshop*, pp. 54-62, 2007.
- [7] J.J. Boutros, E. Calvanese, and A. Guillén i Fàbregas, "Turbo code design for block fading channels," *Allerton Conf. on Communication and Control*, Illinois, 2004.
- [8] J.J. Boutros, A. Guillén i Fàbregas, and E. Calvanese, "Analysis of coding on non-ergodic block fading channels," *Allerton Conf. on Communication and Control*, Illinois, 2005.
- [9] J.J. Boutros, A. Guillén i Fàbregas, E. Biglieri, and G. Zémor, "Low-Density Parity-Check Codes for Nonergodic Block-Fading Channels," *IEEE Trans. on Inf. Theory*, submitted Oct. 2007, Download from arxiv.org
- [10] T.M. Cover and J.A. Thomas, *Elements of Information Theory*, New York, Wiley, 1991.
- [11] T. Cover and A.E. Gamal, "Capacity theorems for the relay channel," *IEEE Trans. on Inf. Theory*, vol. 25, no. 5, pp. 572-584, Sep. 1979.
- [12] A. Guillén i Fàbregas, *Concatenated codes for block-fading channels*, Ph.D. thesis, EPFL, June 2004.
- [13] A. Guillén i Fàbregas, and G. Caire, "Coded modulation in the block-fading channel: coding theorems and code construction," *IEEE Trans. on Inf. Theory*, vol. 52, no. 1, pp. 91-114, Jan. 2006.
- [14] J. Ha, J. Kim, and S.W. McLaughlin, "Rate-Compatible Puncturing of Low-Density Parity-Check Codes," *IEEE Trans. on Inf. Theory*, vol. 50, no. 11, pp. 2824-2836, Nov. 2004.
- [15] J. Hagenauer, "Rate-compatible punctured convolutional codes (RCPC codes) and their applications," *IEEE Trans. on Commun.*, vol. 36, no. 4, pp. 389-400, Apr. 1988.
- [16] J. Hu and T.M. Duman, "Low Density Parity Check Codes over Wireless Relay Channels," *IEEE Trans. on Wireless Communications*, vol. 6, no. 9, pp. 3384-3394, Sep. 2007.
- [17] T.E. Hunter, *Coded cooperation: a new framework for user cooperation in wireless systems*, Ph.D. thesis, University of Texas at Dallas, 2004.
- [18] A. Nosratinia and T.E. Hunter, "Diversity through coded cooperation," *IEEE Trans. on Wireless Communications*, vol. 5, no. 2, pp. 283-289, Feb. 2006.
- [19] T.E. Hunter, S. Sanayei, and A. Nosratinia, "Outage analysis of coded cooperation," *IEEE Trans. on Inf. Theory*, vol. 52, no. 2, pp. 375-391, Feb. 2006.
- [20] R. Knopp and P.A. Humblet, "On coding for block fading channels," *IEEE Trans. on Inf. Theory*, vol. 46, no. 1, pp. 189-205, Jan. 2000.
- [21] G. Kramer, I. Marić, and R.D. Yates, *Cooperative Communications*, Foundations and Trends in Networking, Hannover MA, NOW publishers, June 2007.

- [22] J.N. Laneman, *Cooperative Diversity in Wireless Networks: Algorithms and Architectures*, Ph.D. thesis, M.I.T., Cambridge, MA, 2002.
- [23] J.N. Laneman, D. Tse, and G.W. Wornell, "Cooperative diversity in wireless networks: Efficient protocols and outage behavior," *IEEE Trans. on Inf. Theory*, vol. 50, no. 12, pp. 3062-3080, Dec. 2004.
- [24] A. Lapidoth, "The performance of convolutional codes on the block erasure channel using various finite interleaving techniques," *IEEE Trans. on Inf. Theory*, vol. 40, no. 5, pp. 1459-1473, Sep. 1994.
- [25] J. Li and K. Narayanan, "Rate-compatible low-density parity-check codes for capacity-approaching ARQ scheme in packet data communications," *Int. Conf. on Comm., Internet, and Info. Tech.(CIIT)*, pp. 201-206, 2002.
- [26] F.J. MacWilliams and N.J.A. Sloane, *The theory of error-correcting codes*, eight impression (1991), North-Holland, 1977.
- [27] E. Malkamaki and H. Leib, "Evaluating the performance of convolutional codes over block fading channels," *IEEE Trans. on Inf. Theory*, vol. 45, no. 5, pp. 1643-1646, Jul. 1999.
- [28] E.C. van der Meulen, "Three-Terminal Communication Channels," *Advances in Applied Probability*, vol. 3, no. 1, pp. 120-154, 1971.
- [29] A. Nosratinia, T.E. Hunter, and A. Hedayat, "Cooperative communication in wireless networks," *IEEE Communications Magazine*, vol. 42, no. 10, pp. 74-80, Oct. 2004.
- [30] L.H. Ozarow, S. Shamai and A.D. Wyner, "Information theoretic considerations for cellular mobile radio," *IEEE Trans. on Vehicular Technology*, vol. 43, no. 2, pp. 359-379, May 1994.
- [31] P. Razaghi and W. Yu, "Bilayer Low-Density Parity-Check Codes for Decode-and-Forward in Relay Channels," *IEEE Trans. on Inf. Theory*, vol. 53, no. 10, pp. 3723-3739, Oct. 2007.
- [32] T.J. Richardson and R.L. Urbanke, "The capacity of low-density parity-check codes under message-passing decoding," *IEEE Trans. on Inf. Theory*, vol. 47, no. 2, pp. 599-618, Feb. 2001.
- [33] T.J. Richardson and R.L. Urbanke, *Modern Coding Theory*, Cambridge University Press, 2008.
- [34] T.J. Richardson, M.A. Shokrollahi, and R.L. Urbanke, "Design of capacity-approaching irregular low-density parity-checkcodes," *IEEE Trans. on Inf. Theory*, vol. 47, no. 2, pp. 619-637, Feb. 2001.
- [35] T.J. Richardson and R.L. Urbanke, "Multi-Edge Type LDPC Codes," *IEEE Trans. on Inf. Theory*, submitted 2004.
- [36] A. Sendonaris, E. Erkip, and B. Aazhang, "User cooperation diversity. Part I. System description," *IEEE Trans. on Commun.*, vol. 51, no. 11, pp. 1927-1938, Nov. 2003.
- [37] A. Sendonaris, E. Erkip, and B. Aazhang, "User cooperation diversity. Part II. Implementation aspects and performance analysis," *IEEE Trans. on Communications*, vol. 51, no. 11, pp. 1939-1948, Nov. 2003.
- [38] J. Thorpe, "Low-Density Parity-Check (LDPC) codes constructed from protographs," *JPL INP Progress Report*, vol. 42-154, pp. 1-7, Aug. 2003.
- [39] D.N.C. Tse and P. Viswanath, *Fundamentals of Wireless Communication*, Cambridge University Press, May 2005.
- [40] G. Ungerboeck, "Channel coding with multilevel/phase signals," *IEEE Trans. on Inf. Theory*, vol. IT-28, no. 1, pp. 55-67, 1982.
- [41] M. Yazdani and A.H. Banihashemi, "Irregular rate-compatible LDPC codes for capacity-approaching hybrid-ARQ schemes," *Canadian Conf. on Electrical and Computer Engineering*, 2004.
- [42] B. Zhao and M.C. Valenti, "Some new adaptive protocols for the wireless relay channel," *Allerton conference on communication control and computing*, vol. 41, no. 3, pp. 1588-1589, 2003.